Miner Deposita (2016) 51:411–430
DOI 10.1007/s00126-015-0615-y

ARTICLE

The Paleoproterozoic komatiite-hosted PGE mineralization at Lomalampi, Central Lapland Greenstone Belt, northern Finland

T. Törmänen[1] · J. P. Konnunaho[1] · E. Hanski[2] · M. Moilanen[2] · P. Heikura[1]

Received: 3 October 2014 / Accepted: 8 September 2015 / Published online: 1 October 2015

Abstract Several komatiite-hosted Ni-Cu-PGE deposits occur in Archean and Paleoproterozoic Greenstone Belts in Finland. Some of these deposits are enriched in platinum-group elements, especially in Pd and Pt. The Lomalampi PGE-(Cu-Ni) deposit is associated with a peridotitic cumulate body of the Sattasvaara Formation in the Paleoproterozoic Central Lapland Greenstone Belt. The sulfides in the deposit occur in disseminated form. Whole rock sulfur contents are 0.4–2 wt%, and Ni contents are <0.5 wt% and Cu <0.4 wt%, while PGE contents exceed 500 ppb. The sulfides consist of magmatic pentlandite, pyrrhotite, and chalcopyrite and have not been substantially modified by metamorphic processes. Palladium minerals are associated with sulfides and silicates, but the only Pt-bearing phase, sperrylite, occurs mainly within silicates. The host rock of the deposit is a chromite undersaturated Al-undepleted high-Mg basalt or low-Mg komatiite. In contrast to most other komatiite-hosted Ni-Cu-PGE deposits world-wide that have Pt/Pd around 0.5, the Lomalampi deposit is enriched in Pt over Pd (Pt/Pd=2). Only a weak contamination signal in the host-cumulate is evident in REE data, but a strong signal is evident in S-isotope ratios ($\delta^{34}S$+10‰ to +15‰), which differ substantially from the mantle value (0±2‰). Geochemical characteristics (e.g., PGE enrichment) and R-factor modeling indicate certain similarities between Lomalampi and the Raglan Ni-Cu-PGE deposits of Canada. The combined data suggest that Lomalampi formed through contamination of a PGE-rich magnesian magma with S rich country rocks. This suggests that the extensive Central Lapland Greenstone Belt is favorable for komatiite-hosted Ni-Cu-PGE deposits, which are substantially enriched in platinum and palladium.

Keywords Platinum-group elements · PGEs · Komatiite · Disseminated sulfide deposit · Paleoproterozoic · Lapland · Finland

Editorial handling: W. Maier

Electronic supplementary material The online version of this article (doi:10.1007/s00126-015-0615-y) contains supplementary material, which is available to authorized users.

✉ T. Törmänen
tuomo.tormanen@gtk.fi

J. P. Konnunaho
jukka.konnunaho@gtk.fi

M. Moilanen
Marko.Moilanen@oulu.fi

P. Heikura
pertti.heikura@gtk.fi

[1] Geological Survey of Finland, Box 77, 96101 Rovaniemi, Finland

[2] University of Oulu, Oulu, Finland

Introduction

Komatiite-hosted Ni-Cu deposits are important sources for Ni and Cu. Some of them also contain significant amounts of PGE, especially Pd and Pt, such as the Ni-Cu deposits associated with komatiitic basalts in the Paleoproterozoic Raglan Belt, Canada (e.g., Lesher 2007). In komatiitic systems, high concentrations of PGE (>500 ppb) commonly occur in sulfur-rich ores (S>5 wt%), whereas disseminated and sulfur-poorer (S<5 wt%) ores are usually low in PGE (e.g., Naldrett 2004). Some sulfur-poor and PGE-enriched occurrences have been described from differentiated komatiitic bodies in Canada and Western Australia (e.g., Stone et al. 1996; Fiorentini et al. 2007; Locmelis et al. 2009), but they have little economic importance.

Several komatiite-hosted Ni-Cu-(PGE) deposits and occurrences are known to occur in Archean and Paleoproterozoic

Greenstone Belts in eastern and northern Finland (e.g., Heggie et al. 2013; Konnunaho et al. 2013; Finnickel public database, GTK). These deposits are mainly disseminated with a relatively low S content (S<5 wt%), but some of them also contain massive sulfide accumulations (e.g., Hietaharju, Peura-aho, and Tainiovaara) (Konnunaho et al. 2015). Several deposits, including the Archean Vaara, Hietaharju, and Peura-aho deposits in the Suomussalmi Greenstone Belt and the Paleoproterozoic Lomalampi deposit in the Central Lapland Greenstone Belt (CLGB), are of potential economic interest due to their elevated PGE (Pd+Pt>500 ppb) contents. In common with most disseminated komatiite-hosted Ni-Cu-(PGE) deposits (i.e., type II of Lesher and Keays 2002) worldwide, most of the Finnish deposits are enriched in palladium over platinum, whereas the Lomalampi mineralization is enriched in platinum over palladium. Platinum-dominant PGE enrichments are also associated with some sulfide-poor komatiite-hosted stratiform "reef"-type occurrences (i.e., type III of Lesher and Keays 2002) and in reef-type deposits in layered intrusions (Maier 2005).

The Paleoproterozoic Lomalampi deposit is characterized by relatively high Pt/Pd (approximately 2.0), which exceeds the chondritic value. This feature is unusual amongst komatiite-hosted Ni-Cu-(PGE) deposits worldwide. Lomalampi is also unusual in having relatively high PGE/(Ni+Cu).

In this article, we describe the Lomalampi deposit, focusing on petrological and geochemical features of the associated komatiitic rocks and the chalcophile element geochemistry of the deposit. We discuss the genesis of the deposit, its unique Pt/Pd ratio, PGE enrichment in this, and some other Ni-Cu-PGE deposits nearby, and possible processes responsible for these features.

Geological setting

The Central Lapland Greenstone Belt (CLGB) constitutes the main part of a large Greenstone Belt extending some 400 km from the Russian border in the east to the Norwegian coast in the north (Fig. 1). The Paleoproterozoic evolution of the Central Lapland Greenstone Belt started at ca. 2.5 Ga with rifting of the Archean basement followed by sedimentation and mafic magmatism in an intracratonic to cratonic margin rift setting. This stage ended at ca. 2.0 Ga (e.g., Lehtonen et al. 1998; Hanski and Huhma 2005). The rift phase was followed by multiple compressional stages and associated felsic and mafic magmatism related to the Svecofennian orogenic events between 1.91 and 1.80 Ga (e.g., Lehtonen et al. 1998; Hölttä et al. 2007). The youngest supracrustal sequences were deposited between 1.88 and 1.77 Ga in a molasses environment (Simonen 1980; Hanski et al. 2001b). In this paper, we focus on geological formations belonging to the Savukoski Group, as this contains the majority of komatiitic rocks of the CLGB, including the host rocks of the Lomalampi PGE-Ni-Cu-Au mineralization. For a more comprehensive description of the CLGB, the reader is referred to the works of Lehtonen et al. (1998), Hanski et al. (2001b), and Hanski and Huhma (2005).

In the Lomalampi area, the bedrock consists dominantly of various clastic sedimentary rocks and ultramafic volcanic rocks belonging to the Sodankylä and Savukoski Groups, respectively (Fig. 2). Major intrusive phases are represented by the 2.44-Ga Koitelainen mafic layered intrusion to the south and the 1.77-Ga post-orogenic granites to the north of the study area (Huhma 1986; Mutanen and Huhma 2001). Further to the south, there are several mafic-ultramafic intrusions and sills, most notably the 2.05-Ga Kevitsa and Sakatti intrusions, both of which host magmatic Ni-Cu-PGE deposits (Maier et al. 2015). The Sodankylä Group is mostly composed of quartzites and mica schists deposited in a shallow marine setting and lesser amounts of mafic volcanic rocks (Lehtonen et al. 1998; Hanski and Huhma 2005). The lowermost units of the Savukoski Group, deposited on top of the Sodankylä Group, are composed of fine-grained metasedimentary rocks, typically phyllites and black schists with subordinate greywackes and mafic tuffites, and minor dolomites (i.e., Matarakoski Formation). Since no stratigraphic break has been observed between the two groups, the deposition of these finer-grained sediments indicates deepening of the depositional basin (Hanski and Huhma 2005). In the western part of the CLGB, the metasediments are overlain by mafic volcanic rocks of the Linkupalo Formation, followed by more primitive komatiitic and picritic volcanic rocks (Sattasvaara and Sotkaselkä Formations, respectively). The Lomalampi area is dominated by komatiites and komatiitic basalts belonging to the Peurasuvanto Formation, which is correlative to the Sattasvaara Formation, while mafic volcanic rocks are rare and picrites are absent.

Ultramafic volcanic rocks in the Lomalampi area comprise fine-grained lavas, breccias, tuffs, and various types of hyaloclastic rocks. Associated cumulate rocks are mostly fine- to medium-grained olivine orthocumulates with subordinate amounts of pyroxenitic cumulates, olivine- and pyroxene-phyric lavas, and gabbros. The most abundant metasedimentary rocks are phyllites, black schists, greywackes, and quartzites, most of which are interpreted as belonging to the Matarakoski Formation.

The age of the Savukoski Group is constrained by the U-Pb zircon ages of the crosscutting 2058±4 Ma Kevitsa mafic layered intrusion and a 2048±5 Ma quartz porphyry (Mutanen and Huhma 2001; Räsänen and Huhma 2001; Hanski and Huhma 2005). Hanski et al. (2001a) used clinopyroxene-whole rock pairs from komatiitic rocks in the

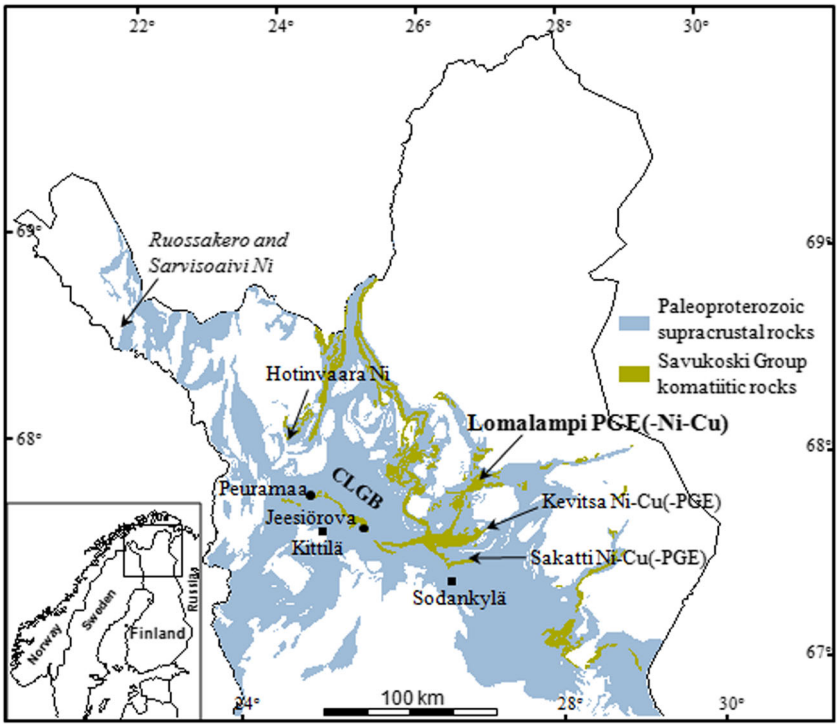

Fig. 1 Location of the Lomalampi deposit within the Central Lapland Greenstone Belt (*CLGB*). Also indicated are other *Archean* and Proterozoic komatiite-hosted Ni and intrusion-hosted Ni-Cu(−PGE) deposits, as well as previously studied occurrence of komatiites (*black dots*, Hanski et al. 2001a)

Jeesiörova area in Kitttilä for Sm-Nd isotope dating and obtained an age of 2056±25 Ma, which represents the best currently available age estimate for the komatiites of the Savukoski Group.

Metamorphism and deformation

Hölttä et al. (2007) divided the CLGB into six (I–VI) metamorphic domains. The Lomalampi area belongs to the mid-amphibolite facies zone II. However, the metamorphic mineral paragenesis of mafic-ultramafic rocks (serpentine-chlorite± amphibole) is similar to that seen in rocks in the Kittilä area, as described by Hanski et al. (2001a), and indicates greenschist to lower amphibolite facies conditions.

Hölttä et al. (2007) determined three ductile deformation phases in the central part of the CLGB. Early deformation phases, D1+D2, are thought to be related to horizontal thrust tectonics, resulting in flat-lying to subhorizontal folds and foliations. A later D3 phase overprints earlier structures. It is characterized by folds with highly variable axial strikes and dips. It also reactivated earlier thrusts and generated high-strain shear zones. In the Lomalampi area, most recorded fold axes are NE-SW-trending with subhorizontal to shallow plunges. These are probably related to D3 events, although downward younging observations from metasediments in the central part of the study area indicate possibly overturned folds related to D2 thrust tectonics. There are several NE-SW-trending shear zones, which are usually located at the contacts of the cumulate bodies (Fig. 2) and possibly also some NW-SE-trending faults (c.f. Hölttä et al. 2007). However, the local structural features are poorly defined and understood.

Sampling and analytical methods

Samples for whole-rock analyses from the Lomalampi area were collected from 44 drill cores (Fig 2), which were obtained during a research program of the Geological Survey of Finland between 2004 and 2008. Split drill core samples used for petrological analyses varied generally from 10 to 50 cm in length, while samples for base and precious metal analyses varied from 1 to 2 m in length.

All drill core analyses were performed by the geochemical laboratory of GTK and Labtium Oy (former geochemical laboratory of GTK). Petrological samples were pulverized using carbon steel bowl. Whole-rock analyses for major elements and selected trace elements were performed by X-ray fluorescence (XRF) on pressed powder pellets. Samples for rare earth elements were digested with HF-$HClO_4$—digestion, followed by Li-metaborate—sodium perborate fusion and analyzed by inductively coupled plasma mass spectrometry (ICP-MS). Base metals analyses (14 elements) were carried out with partial dissolution by aqua regia followed by inductively coupled plasma optical emission spectrometry (ICP-OES) with the detection levels varying from 1 to 50 ppm. Platinum, palladium, and gold were determined by Pb fire assay followed by ICP-OES (10 ppb detection limit for all three elements). A number

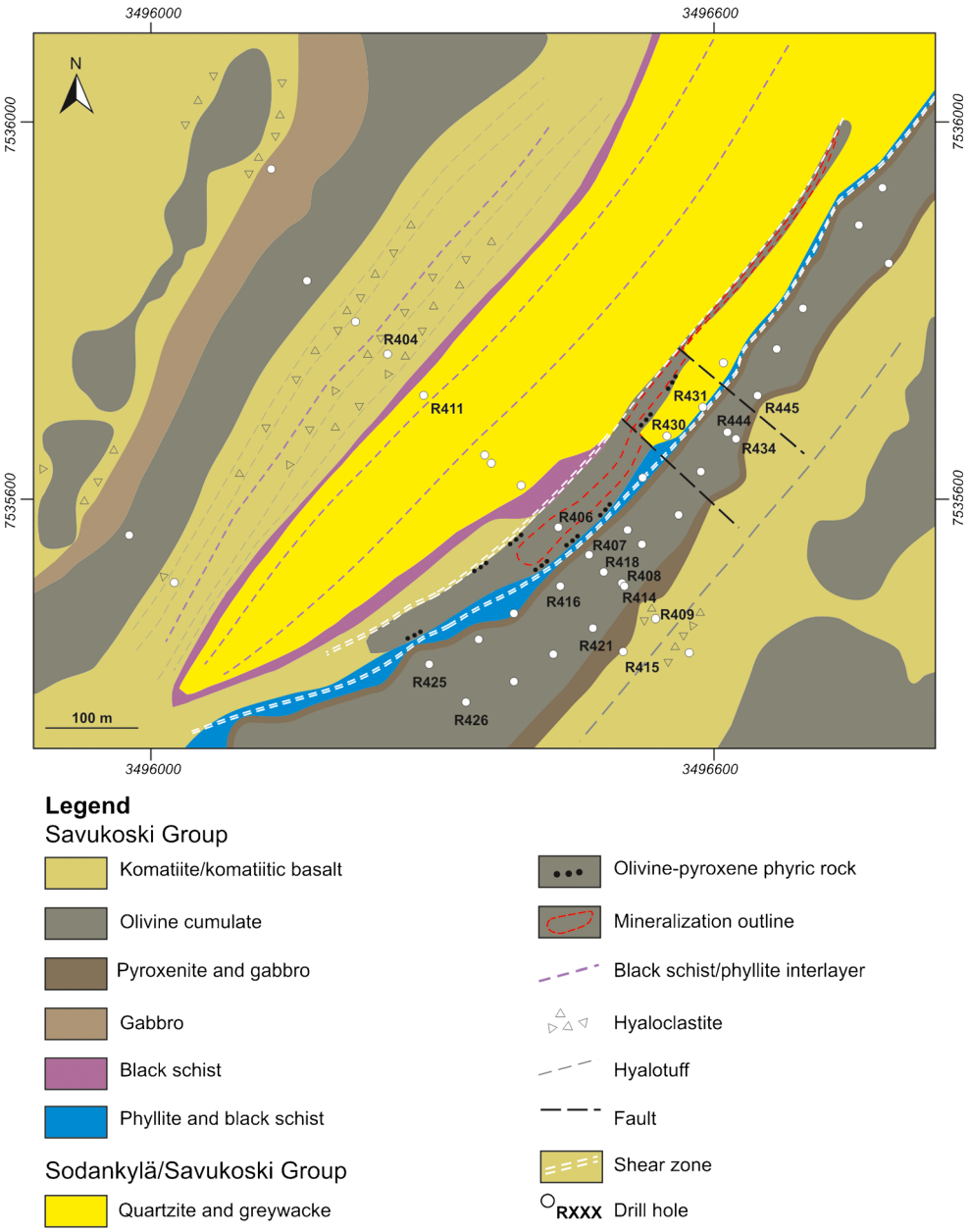

Fig. 2 Geological map of the Lomalampi area. *White dots* indicate DDH collar points, and *numbered collars* are referred in the text

of samples were analyzed for Au and six platinum group elements by ICP-MS coupled with NiS fire assay and Te coprecipitation (detection limits in ppb: Au 0.5, Pd 1, Pt 0.1, Rh 1, Ir 0.1, Ru 2, and Os 1). The method was described by Juvonen et al. (2002).

In order to estimate the amount of silicate-bound nickel in the ICP-OES analyses, six drill core samples were dissolved using bromine methanol (BrMeOH) leaching, followed by determination of nickel by flame atomic absorption (FAAS). Powders of the same samples were also dissolved in aqua regia followed by ICP-OES determination of nickel. The difference in analyzed Ni contents between the bromine methanol and aqua regia leaches varies from 0 to 400 ppm, depending on the S and Ni content of the samples, as well as the type and degree of alteration: The least altered samples dominated by serpentine show the largest difference between the aqua regia and BrMeOH leaching, i.e., highest contents of silicate-bound Ni in the ICP-OES analyses, whereas more altered samples consisting mainly of talc and carbonate show nearly identical Ni contents with both leaching methods. Based on this observation, a 400-ppm reduction from the analyzed Ni concentrations was made before calculating the Ni content in the sulfide fraction.

Sulfur isotopes were determined in four whole-rock and hand-picked sulfide samples. The whole-rock sulfur isotope analyses were conducted at the University of Indiana by elemental analyzer-continuous flow isotope ratio mass spectrometry (EA-IRMS) (Studley et al. 2002), while the isotopic

compositions of the hand-picked sulfides were measured at Zymax Forensics Isotope Laboratory (EA-IRMS).

In order to determine the size distribution, hosting phase, and composition of PGM, nine polished thin sections were scanned with a Mineral Liberation Analyzer (MLA, FEI Quanta 600 equipped with EDAX Genesis EDS detector) at the Mineral Processing Laboratory of GTK at Outokumpu. Ten PGE-bearing mineral grains were analyzed (semiquantitative) using a JEOL JSM 5900 scanning electron microscope at the GTK research laboratory in Espoo. An additional MLA study was done on three polished sections made from composite crushed feed (quarter core from six drill holes) used in the metallurgical assessment by the Mineral Processing Laboratory.

Komatiitic rocks of the Lomalampi area

The high-Mg rocks of the Lomalampi area have been divided into three groups on the basis of their geochemical and mineralogical composition and texture: (1) volcanoclastic komatiites, (2) thin komatiite to komatiitic basalt lava flows and their olivine-pyroxene cumulate units (pyroxenites to peridotites), and (3) several bodies of massive cumulates (pyroxenitic to peridotitic and minor gabbroic cumulates), which could represent sills or cumulate zones of thicker lava flows (Fig. 2). The general trend of these cumulates is southwest to northeast. Two major cumulate bodies are located in the southeastern part, while other thinner cumulate bodies occur in the northwestern part of the Lomalampi area. One of the cumulate bodies in the southeastern part of the area hosts the Lomalampi PGE-Cu-Ni mineralization (Fig. 2). The cumulate bodies are mostly composed of serpentine-chlorite±talc±amphibole rocks, with locally developed talc ±carbonate rocks. Serpentine forms pseudomorphs after original cumulus olivine, while chlorite fills the interstitial space. The average diameter of olivine pseudomorphs is 0.5 to 1.0 mm with some elongate grains reaching 4 mm in length. The textures of the cumulate bodies correspond to orthocumulates or mesocumulates. Poikilitic textures are locally preserved with original magmatic pyroxene replaced by amphibole enclosing serpentine pseudomorphs after olivine (Fig. 3).

Various types of ultramafic volcanic rocks occur in the Lomalampi area, especially between the northwest and southeast cumulate bodies. Chemically, their composition varies from komatiitic to komatiitic basalt. They are commonly highly altered and affected by deformation processes, especially at and below the contact with the mineralized cumulates. Based on drill core observations, the rocks represent tuffs, hyaloclastites and other fragmental rocks (Fig. 3a), as well as lava flows 5 to 10 m thick. Some of these flows contain olivine-phyric or relatively melt-rich orthocumulate zones. Thin (0.5 to 3 m) komatiitic to komatiitic basalt dikes occur mostly in the narrow interval between the two major cumulate bodies in the southeast and also cut the more southern, barren cumulate body. The volcanic rocks are generally fine-grained, massive, or sheared rocks composed of variable amounts of amphibole and chlorite with biotite being present in more strongly altered varieties. Locally, hyaloclastites and other fragmental rocks have preserved their original textures, although no primary igneous minerals are preserved.

The mineralized komatiitic cumulate is a sheet-like body dipping at an angle of 80° to the southeast. The ore-bearing body has been delineated by diamond drilling to be approximately 700 m long along strike and possibly extending both toward the southeast and northwest. The calculated true thickness ranges mostly from 30 to 65 m, being greater in the deeper intersections. Toward the northwest, the mineralized cumulate becomes significantly thinner, ranging from 10 to 20 m in thickness in shallower parts, while the deeper intersections are around 40 m thick. In the most northwestern part, the depth extension and thickness of the mineralized cumulate are still uncertain, as it has been intersected by a limited number of drill holes at relatively shallower levels.

In the mineralized cumulate, the degree of alteration increases toward the structural footwall with increasing amounts of talc± carbonate resulting in a zone of talc or talc-carbonate rock with a thickness from a few meters to 20 m. Variable amounts of thin talc-carbonate veins, commonly with some remobilized sulfides, are a ubiquitous feature of the mineralized cumulate. Drill core and thin section observations indicate the presence of a "white spotted" rock type, which is composed of rotated, possibly porphyroblastic amphibole (Fig. 3e–f) as well as talc and carbonate grains in a fine-grained, sheared, and schistose chlorite-talc-amphibole matrix. This rock type occurs mostly as 1- to 10-m-thick zones at the structural upper contact of the cumulate and more rarely also at the lower contact of the cumulate. It could represent an originally pyroxene-olivine-phyric rock. The footwall and hanging wall contacts are usually tectonized and composed of a 0.5- to 3-m-thick amphibole-chlorite±biotite schist zone. The footwall rock package consists of black schists, phyllites, and komatiitic to komatiitic basaltic volcanic rocks, all of which are schistose and variably deformed and also commonly sheared. The type of immediate footwall rock varies even between drill holes in the same profile, resulting from faulted and sheared footwall contacts. Toward the northeast, the narrower cumulate body is often bordered by quartzites, greywackes, and phyllites. The abrupt thinning of the cumulate body combined with a change in the nature of the footwall and hanging-wall lithologies indicate the presence of fault and/or shear zones.

The mineralized cumulate and the southern barren cumulate bodies are separated from each other by a narrow, heterogeneous rock package consisting of phyllite, black schist, komatiitic, and komatiitic basaltic volcanic rocks and dikes. The distance between the two cumulate bodies varies generally from 5 to 40 m in drill cores, increasing to more than 50 m in the northeastern part.

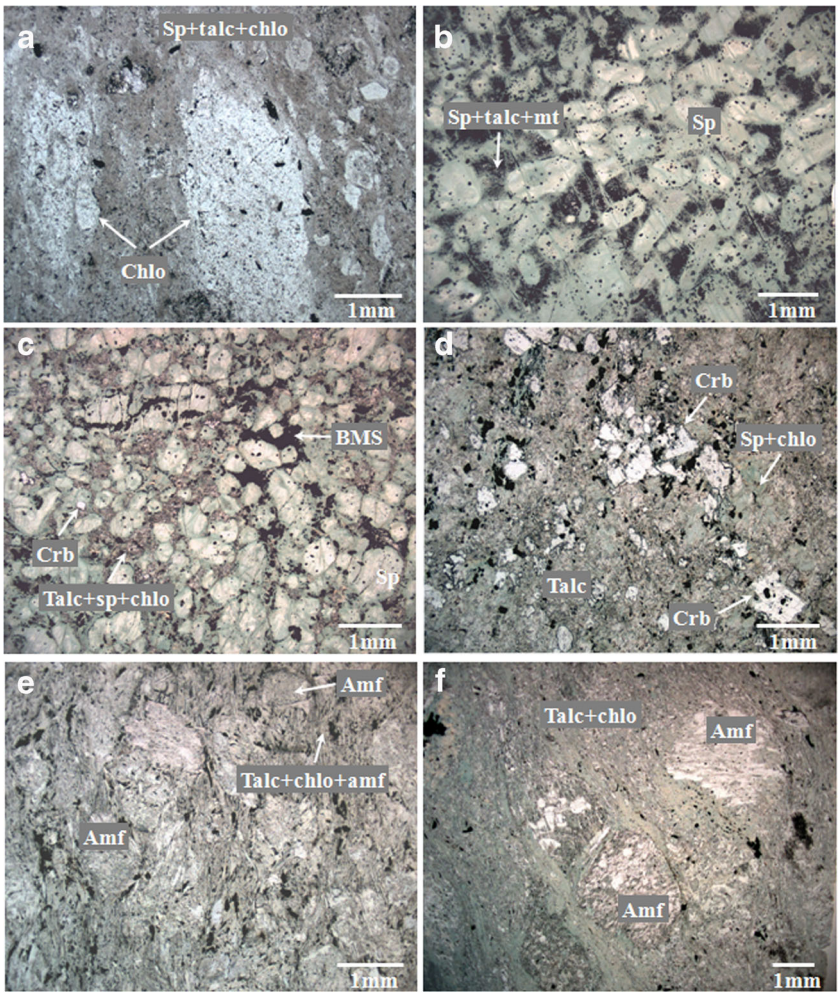

Fig. 3 Photomicrographs showing textures of various komatiitic rocks from Lomalampi. **a** Hyalo tuff with variable-sized chlorite-altered fragments in a fine-grained serpentine-talc-chlorite matrix. **b** Non-mineralized ore cumulate showing well-preserved orthocumulate textures with serpentine replacing olivine and serpentine-talc+magnetite replacing interstitial material. **c** Weakly mineralized ore cumulate with well-preserved textures. *Black patches* are composed of base metal sulfides. **d** Talc-carbonate altered lower part of ore cumulate. **e** Uppermost part of ore cumulate (white-*spotted type*) with mm-sized porphyroblast-like amphibole in a sheared talc-chlorite-amphibole matrix. **f** *White-spotted cumulate type* from the footwall contact of the ore cumulate. *Chlo* chlorite, *Sp* serpentine, *Mt* magnetite, *Crb* carbonate, *BMS* base metal sulfides, *Amf* amphibole

The southern barren cumulate has a similar 80° dip toward the southeast as the mineralized cumulate. The whole cumulate body has a thickness of about 100 m and a strike length of at least 800 m (Fig. 2). Here, talc-carbonate alteration is much less abundant and less penetrative compared to the mineralized cumulate, and talc-carbonate veins are less abundant. The major difference between the two cumulate bodies is the pyroxenite-gabbro zone occurring at the upper and lower contacts of the barren cumulate. Typically, it consists of a pyroxenitic inner zone a few meters in thickness followed by an approximately 10-m-thick gabbroic outer zone. The transition from the inner olivine cumulate to pyroxenitic and gabbroic rocks can be sharp or gradational.

The Lomalampi PGE-Cu-Ni deposit

The Lomalampi deposit is a PGE-rich, disseminated Fe-Ni-Cu sulfide mineralization hosted by an olivine orthocumulate body (Fig. 4). In the classification scheme of Lesher and Keays (2002), it belongs to the IIb or IIc type deposits (strata-bound internal). The NE-SW-trending mineralization has been traced by drilling for ~550 m along strike to a maximum depth of 130 m. The thickness of the mineralization varies greatly even between drill holes of the same profile: generally one to three relatively higher-grade (>500 ppb combined Pt and Pd) intervals occur within a thick PGE-anomalous zone (>100 ppb). The thickness of the high-grade intersections ranges from 1 m to more than 10 m, while the lower-grade envelope can be up to 40 m thick (Fig. 5). High-grade PGE-mineralization is usually encountered in the lower or middle part of the olivine cumulate sheet, but it can also occur in the upper part. Thin, 1 to 4-m-thick PGE-enriched (100–400 ppb) intervals also occur in the otherwise non-mineralized southwestern part of the host cumulate, in the southern cumulate body ("barren cumulate") and also in gabbroic rocks associated with olivine cumulates in the northwestern part of the study area. The mineral resource estimate produced by GTK contains 3.06 million t at 0.269 ppm Pt, 0.122 ppm Pd, 0.074 ppm Au, 0.1682 wt% Ni (including some silicate-bound nickel),

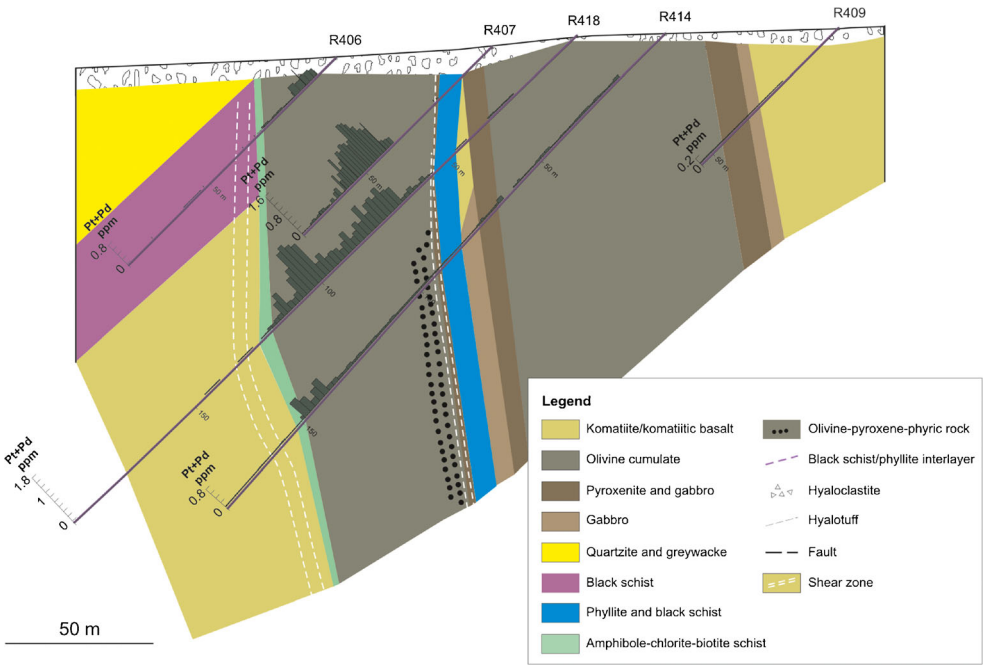

Fig. 4 Vertical section showing the ore cumulate and barren cumulate and their immediate wall rocks with drill cores and their Pt+Pd contents. For location, refer to the drill core numbering shown on Fig. 2

and 0.0571 wt% Cu, at a cutoff of 0.1 ppm Pt (Koistinen and Heikura 2010; Törmänen et al. 2010; Eilu et al. 2013).

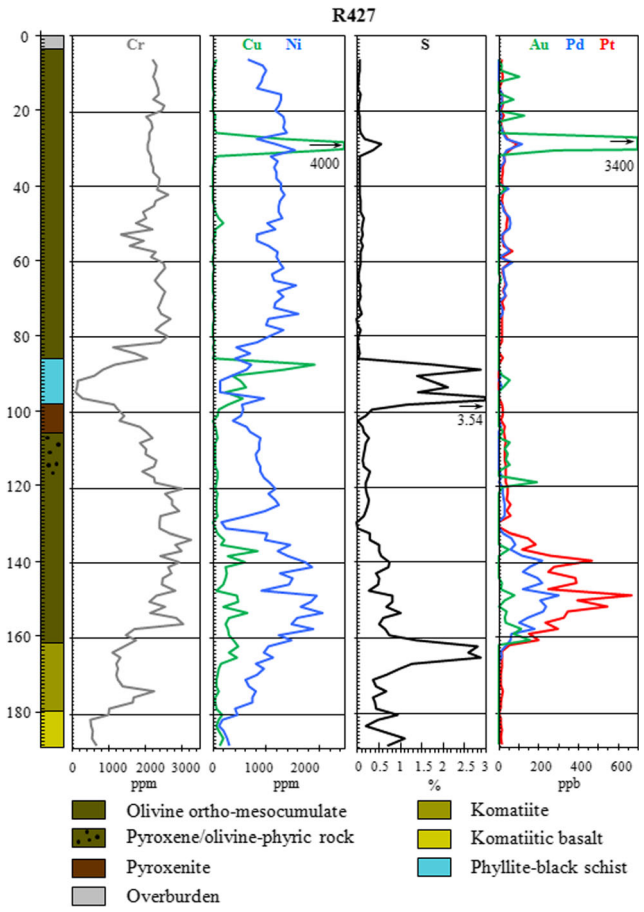

Fig. 5 Cr, Cu, Ni, S, Au, Pd, and Pt contents in drill core R427 (indicated on the map of Fig. 2)

Disseminated sulfides occur as small (Ø 0.01–0.5 mm) single or composite grains (Fig. 6f), or as slightly larger (Ø 0.5 mm), lobate aggregates of intergrown sulfides and platy serpentine (i.e., trellis texture, Barnes and Hill 2000), similar to those found in many other komatiite-hosted disseminated sulfide deposits (e.g., Barnes et al. 2009) (Fig. 6a–c). Some more sulfide-rich samples have coarser-grained sulfides and sulfide blebs commonly 1 to 2 mm and locally up to 5–8 mm in diameter, with more granular and/or annealed textures (Fig. 6d, e). Sulfides together with magnetite also occur in millimeter- to centimeter-thick talc-carbonate veins.

The sulfide paragenesis represents a typical magmatic sulfide assemblage consisting of pyrrhotite, pentlandite, and chalcopyrite with pyrrhotite being by far the most abundant sulfide phase. Magnetite occurs in variable amounts with sulfides, commonly concentrated along the outer edges of sulfide aggregates, and in some cases, partially replacing base metal sulfides (Fig. 6d). In As-bearing samples, trace amounts of subeuhedral sulfarsenides (cobaltite-gersdorfite-arsenopyrite) and, locally, nickeline together with trace löllingite are present. Trace phases found by MLA and SEM include pyrite, sphalerite, millerite, galena, and molybdenite. Despite the altered nature of the host rock and the presence of more strongly altered talc and talc-carbonate rocks, pyrite and millerite are very rare minerals at Lomalampi.

Occurrence of PGM

So far, no systematic study of the distribution of platinum-group elements between different mineral phases has been conducted for the Lomalampi mineralization. Nevertheless,

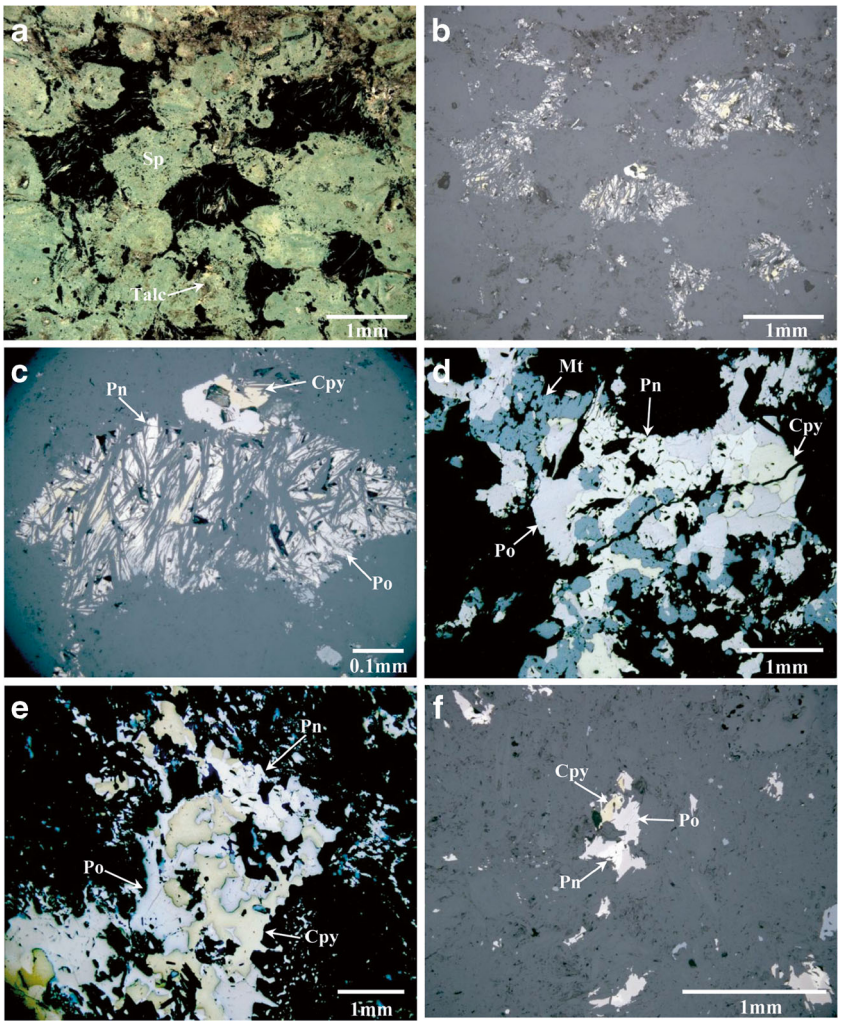

Fig. 6 Photomicrographs of sulfide textures. **a** Interstitial sulfides between serpentine-altered cumulus olivine. **b** Same as previous, incident light. **c** Close-up of B showing the intergrown nature of sulfides with secondary silicates (serpentine). **d** More coarse-grained, recrystallized sulfides, rimmed with, and partially replaced by later magnetite. **e** Coarse-grained, recrystallized sulfides. **f** More fine-grained, sparsely disseminated sulfides associated with advanced talc-carbonate alteration. *Sp* serpentine, *Pn* pentlandite, *Cpy* chalcopyrite, *Po* pyrrhotite, *Mt* magnetite

some information has been obtained from MLA scanning of nine polished thin sections from five different drill holes. Additional SEM investigations were conducted on seven of these thin sections. The MLA scans located 301 Pd-bearing, 450 Pt-bearing, and 4 Ru-bearing grains, and the SEM studies further indicated the presence of a Rh-containing phase. Platinum-group minerals (PGMs) occur as very small grains associated with various base metal sulfides, MeAsS-MeAs phases, silicates, oxides, and carbonates (SEM-images presented in the Electronic Supplementary Materials ESM 1). The average grain size of the PGM is between 4 and 6 μm, whereas the largest grains measure 20 to 30 μm. The mineralogy of Pt- and Pd-rich phases is surprisingly simple: Palladium occurs as three discrete Pd-Ni-Te±Sb±Bi phases, while the only Pt mineral found is sperrylite ($PtAs_2$). Table 1 shows semiquantitative SEM-EDS analyses of various Pd-rich phases and sperrylite. Of the three Pd-bearing phases, two are Ni-dominant. The first four analyses in Table 1 probably represent Bi-bearing palladian melonite $(Ni,Pd)(Te,Bi)_2$. Melonite and merenskyite ($PdTe_2$) form a complete solid solution series and can contain highly variable amounts of bismuth, but only negligible amounts of Sb (Cabri and LaFlamme 1981; Barkov et al. 2002; Gervilla and Kojonen 2002). The two other phases are similar to unnamed Ni-Pd minerals described by Chen et al. (1993), Augé et al. (2002), and Barkov et al. (2002). The only Rh-bearing PGM found by SEM occurs as four micrometer-sized, exsolution-like grains in a small cobaltite grain associated with base metal sulfides. Similar Ru-bearing exsolutions were also observed in cobaltite from another sample.

Based on MLA studies, approximately 80 % of sperrylite grains and 50 % of Pd minerals are hosted by silicates, but there is some variation between different samples, with as much as 71 % of Pd minerals occurring with base metal sulfides in some samples. However, the possible occurrence of Pt and Pd in base metal sulfides or sulfarsenides was not determined.

Whole-rock geochemistry

Representative examples of whole-rock major and trace element compositions of various types of komatiitic rocks from

Table 1 Selected PGM analyses from the Lomalampi deposit

Phase	Fe	Ni	Pd	Pt	As	Bi	Sb	Te	Total
Melonite	4.7	24.5	6.5	n.d.	n.d.	3.8	n.d.	60.5	100.00
Melonite	6.5	14.3	7.1	n.d.	n.d.	3.1	n.d.	59.0	100.00
Melonite	6.4	24.0	7.6	n.d.	n.d.	4.1	n.d.	57.9	100.00
Melonite	4.7	24.5	6.5	n.d.	n.d.	3.8	n.d.	60.5	100.00
$(Ni,Pd)_{1+x}(Te,Sb,Bi)_{1-x}$	1.6	28.2	7.7	n.d.	n.d.	3.4	12.4	46.8	100.00
$(Ni,Pd)_{1+x}(Te,Sb,Bi)_{1-x}$	1.6	28.1	7.2	n.d.	n.d.	3.3	12.9	46.9	100.00
$(Pd,Ni)_3(Te,Sb)_4$	n.d.	20.1	23.7	n.d.	n.d.	n.d.	27.6	28.6	100.00
$(Pd,Ni)_3(Te,Sb)_4$	n.d.	19.8	23.6	n.d.	1.4	n.d.	27.2	28.0	100.00
Sperrylite	5.2	n.d.	n.d.	31.3	63.5	n.d.	n.d.	n.d.	100.00
Sperrylite	4.6	n.d.	n.d.	31.2	64.2	n.d.	n.d.	n.d.	100.00

Values are in atomic percent

n.d. not detected

the Lomalampi area are provided in Table 2. Most of the cumulate bodies are orthocumulates to mesocumulates, whereas olivine adcumulates are absent. Other komatiitic rocks in the area comprise a heterogeneous group of komatiitic lava flows and associated thin olivine-pyroxene cumulate bodies, and volcanoclastic komatiites.

The barren cumulate bodies contain a group of particularly MgO-rich cumulates (MgO>35 wt%), which are absent in the mineralized cumulate body. ESM 2 in the ESM displays TiO_2 and Al_2O_3 contents of mineralized and barren komatiitic cumulate bodies plotted against their MgO contents. They show that TiO_2 and Al_2O_3 contents in the two types of cumulates are nearly similar, whereas other komatiitic rocks in study area, such as hyaloclastites, have higher TiO_2 and lower Al_2O_3 contents. As shown in Fig. 7a, the highest Cr contents were determined for peridotites with high MgO contents in the barren cumulate bodies. At lower MgO contents, both the barren and mineralized cumulates contain similar Cr contents. There are no significant differences in the Cr contents between komatiitic flows and cumulate bodies with similar MgO contents, and all rocks form a consistent trend of increasing Cr with increasing MgO, representing cotectic olivine-chromite crystallization. Nickel contents of komatiitic rocks at Lomalampi also show a positive correlation with MgO from gabbroic cumulates to peridotitic cumulates. The highest Ni contents occur in peridotitic samples from the barren cumulate body, which also contains the most MgO-rich peridotites. The most MgO-rich cumulates from the mineralized cumulate body are slightly depleted in Ni compared to barren cumulates (Fig. 7b).

Based on the Al_2O_3/TiO_2 ratio, the cumulate bodies are mostly of the Al-undepleted type komatiite (i.e., AUK or Munro-type, Arndt 2008) (Al_2O_3/TiO_2>15), with barren cumulate bodies having slightly higher Al_2O_3/TiO_2 ratios than the mineralized cumulates. Komatiites and komatiitic basalts belong to the Ti-enriched type (i.e., Karasjok type, Barnes and Often 1990; Barley et al. 2000) (Al_2O_3/TiO_2<15). The average $(Gd/Yb)_{PM}$ ratios for various komatiitic rocks in the Lomalampi area fall between 1.28 and 1.61, being close to the ratio of Al-depleted type komatiite (i.e., ADK or Barberton-type, Arndt 2008), with the highest $(Gd/Yb)_{PM}$ ratios associated with extrusive rocks (flows, hyaloclastites, etc.). Based on Hanski et al. (2001a), similarly high $[Gd/Yb]_{PM}$ ratios are typical for Paleoproterozoic komatiitic rocks in the Jeesiörova area of the Savukoski Group in the CLGB. The $[Al_2O_3]$ and $[TiO_2]$ (Hanski 1992) values of all Lomalampi komatiitic rocks also show that the cumulate bodies represent AUK, whereas komatiites and komatiitic basalts in the area were generated from a Ti-enriched komatiite magma.

Figure 8a shows chondrite-normalized REE patterns for a barren cumulate body. Some of the samples are clearly enriched in LREE, whereas others have flat or only slightly LREE-depleted patterns ($(La/Sm)_{CN}$ is around 1). The HREE patterns vary from nearly flat to slightly depleted in both types (average $(Gd/Yb)_{CN}$ is around 1.2 to 1.3). Figure 8b shows chondrite-normalized REE patterns of the mineralized cumulate body (S<0.2 wt%), which show variable LREE depletions ($(La/Sm)_{CN}$ is around 0.5) and similar HREE patterns to those of the barren cumulate. The REE patterns of the volcanoclastic komatiites and other komatiitic to komatiitic basalts in the Lomalampi area are variable, but mostly similar to the hump-shaped REE patterns of uncontaminated komatiites in the Jeesiörova and Sattasvaara areas (Fig. 8c) (Lehtonen et al. 1998; Hanski et al. 2001a; and unpublished geochemical data of Geological Survey of Finland), although komatiitic cumulates of the Lomalampi area have less distinct hump-shaped patterns.

Chalcophile element geochemistry of the Lomalampi deposit

Concentrations of Ni and Cu in mineralized and barren cumulate bodies are generally low (<0.5 wt% Ni, <0.4 wt% Cu, but

Table 2 Selected whole-rock analyses of mineralized cumulate body (MC), barren cumulate body (BC), and surrounding komatiites from the Lomalampi area

Rock type	Prd (BC)	Prd (BC)	Px (BC)	Px (BC)	Gabbro (BC)	Prd (MC)	Prd (MC)	Prd (MC)	Px (MC)	Hyalotuff
DDH	R408	R414	R421	R445	R415	R407	R418	R426	R444	R411
Depth	28.85	51.50	78.00	6.20	151.15	29.20	61.90	124.45	86.65	72.30
SiO_2 (wt%)	41.00	40.80	43.80	46.00	51.5	41.80	43.90	41.70	40.30	39.30
TiO_2	0.21	0.31	0.62	0.33	0.54	0.34	0.31	0.35	0.39	0.54
Al_2O_3	3.74	4.89	8.59	5.59	9.59	5.10	4.99	5.48	5.79	7.37
Cr_2O_3	0.69	0.60	0.27	0.40	0.23	0.59	0.62	0.57	0.46	0.40
FeOtot	10.62	11.11	12.36	8.81	10.36	11.72	13.43	11.72	8.34	10.70
MnO	0.08	0.08	0.14	0.14	0.11	0.08	0.07	0.07	0.15	0.18
MgO	34.70	31.70	18.60	22.20	11.60	29.70	31.70	30.60	23.80	24.70
CaO	0.11	1.95	7.05	8.92	8.27	2.10	1.16	2.30	8.83	5.26
Na_2O	b.d.	b.d.	0.14	b.d.	2.83	b.d.	b.d.	b.d.	b.d.	b.d.
K_2O	<0.01	<0.01	1.96	0.02	1.31	<0.01	<0.01	<0.01	<0.01	0.02
P_2O_5	0.02	0.02	0.04	0.03	0.05	0.02	0.03	0.02	0.03	0.04
Ni (ppm)	1,912	1,713	842	1,270	219	1,275	1,603	1,415	1,327	1,478
Cu	b.d.	b.d.	85	b.d.	b.d.	78	58	b.d.	101	42
S	391	187	1,940	2,011	184	1,600	1,639	622	2,775	763
V	105	105	213	130	248	136	129	148	140	202
Sc	15.5	18.2	31.7	26.8	46.5	21.8	18.2	19.9	24.5	25.8
Sr	b.d.	b.d.	13	10	62	b.d.	b.d.	b.d.	13	98
Ba	b.d.	b.d.	53	24	62	b.d.	b.d.	20	20	b.d.
Rb	b.d.	0.66	b.d.	b.d.	58	0.82	0.55	b.d.	0.71	b.d.
Zr	18	19.5	38	25.7	50	5.83	16.8	24	28.3	25
Hf	n.d.	b.d.	n.d.	0.77	n.d.	b.d.	b.d.	n.d.	0.94	n.d.
Y	3.73	4.02	11.2	8.68	12.4	6.15	5.25	5.36	8.99	6.81
Nb	b.d.	0.85	b.d.	0.84	b.d.	0.7	0.67	b.d.	0.88	n.d.
Zn	125	120	120	89	106	76	89	97	66	198
As	b.d.	b.d.	b.d.	b.d.	b.d.	128	170	55	b.d.	b.d.
Cl	99	92	346	65	447	135	13	109	87	b.d.
U	b.d.	0.21	0.27	b.d.	0.37	0.21	0.26	b.d.	b.d.	b.d.
Th	0.57	b.d.	b.d.	0.5	b.d.	b.d.	b.d.	b.d.	b.d.	b.d.
La	0.37	0.88	1.43	0.41	6.29	0.66	0.99	0.17	0.88	0.43
Ce	1.21	1.5	4.03	1.63	12.9	1.76	1.14	1.11	1.73	1.7
Pr	0.19	0.24	0.68	0.32	1.77	0.27	0.2	0.2	0.29	0.32
Nd	0.95	1.38	3.46	1.91	7.19	1.54	1.12	1.37	1.97	1.9
Sm	0.37	0.41	1.25	0.89	1.95	0.64	0.5	0.52	0.67	0.66
Eu	b.d.	b.d.	0.35	0.12	1.1	b.d.	b.d.	b.d.	0.14	0.33
Gd	0.42	0.62	1.85	1.24	2.47	0.91	0.74	0.71	1.32	1.08
Tb	b.d.	b.d.	0.35	0.21	0.39	0.17	0.13	0.13	0.22	0.19
Dy	0.7	0.57	2.06	1.44	2.11	1.23	0.84	0.86	1.81	1.34
Ho	0.14	0.14	0.43	0.3	0.46	0.21	0.22	0.21	0.35	0.27
Er	0.43	0.44	1.16	0.79	1.37	0.69	0.58	0.57	0.87	0.64
Tm	b.d.	b.d.	0.18	0.11	0.18	b.d.	b.d.	0.11	0.13	0.1
Yb	0.42	0.43	1.12	0.71	1.28	0.73	0.56	0.62	0.67	0.73
Lu	b.d.	b.d.	0.17	0.11	0.17	0.12	b.d.	b.d.	0.1	0.1

b.d. below detection limit, *n.d.* not determined, *BC* barren cumulate, *MC* mineralized cumulate, *Prd* peridotite, *Px* pyroxenite

Pd and Pt concentrations can be relatively high (Pt+Pd> 500 ppb, Table 3). Chalcophile elements (Ni, Cu, Pd, and Pt) show good correlations with S in the mineralized cumulate body (Fig. 9a–b and 10a–b). Correlations between Ni, Cu, and

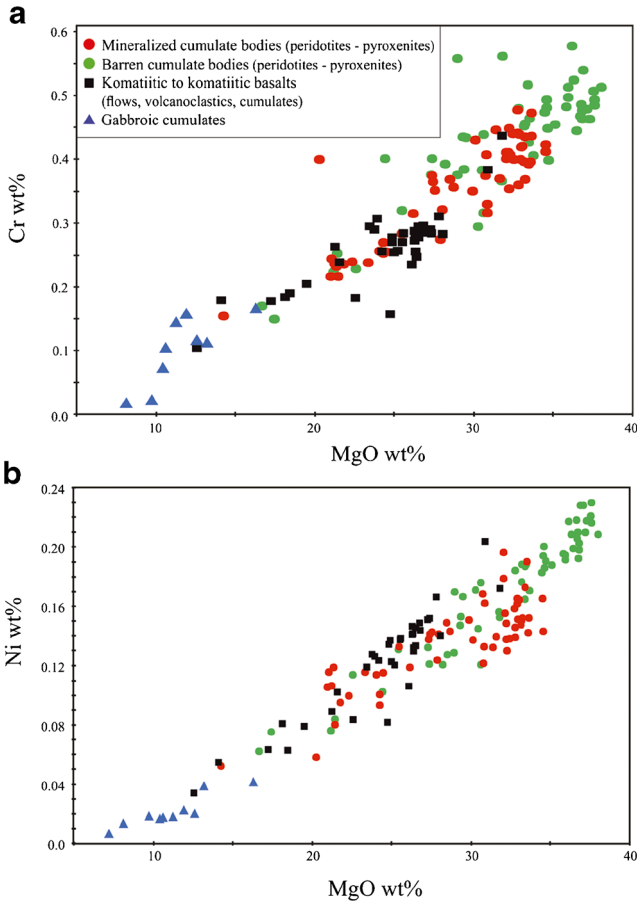

Fig. 7 Whole-rock analyses (S≤2 wt%) from Komatiitic rocks of the Lomalampi area on **a** MgO vs. Cr and **b** MgO vs. Ni diagrams

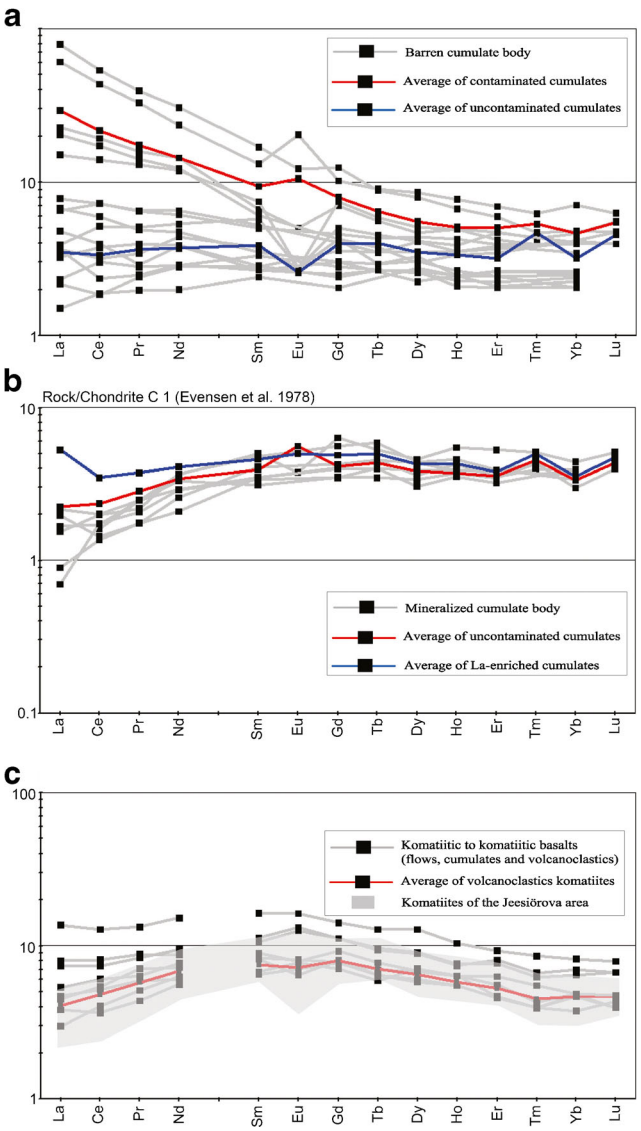

Fig. 8 **a**, **b** Chondrite-normalized REE patterns of barren and mineralized ultramafic bodies and **c** comparison of komatiitic extrusive rocks of the Lomalampi area to komatiitic rocks of the Jeesiörova area. Reference data for the Jeesiörova area taken from Hanski et al. (2001a, b) and unpublished GTK geochemical database

Pt-Pd are also good. There are two distinct trends in the S-Ni diagram, defining different Ni/S ratios (Fig. 9a). These trends are less evident in the S-Cu diagram, which shows a broad positive correlation between S and Cu (Fig. 9b). Figure 10a, b presents S vs. Pd and Pt data. It is noteworthy that most of the Pd- and Pt-enriched samples typically contain less than 2 wt% S, corresponding to the Ni/S=0.2 trend in Fig.9a. There is also a more sulfur-enriched mineralization subtype in the central part of the mineralization (e.g., DDHs R430 and R431 in Fig. 2), but without higher contents of Pd and Pt, corresponding to the Ni/S=0.1 trend in Fig. 9a.

The Ni/Cu ratio varies widely, but most of the samples from the mineralized cumulate body have Ni/Cu ratio from 2 to 10, decreasing with increasing S content (ESM 3). PGE-mineralized samples have Ni/Cu mostly lower than 10 and S contents higher than 0.4 wt%. Some weakly mineralized samples having higher Ni/Cu ratios coupled with low S contents (<0.4 wt%) reflect the effect of the silicate-bound Ni and the presence of minor amounts of Cu (ESM 3).

Palladium and platinum are the most significant ore metals in the Lomalampi deposit, and they show a good correlation with each other. The mineralized samples (S≥0.2 wt%) have an average Pt/Pd ratio of 2.2 (Fig. 11a). Furthermore, continuous PGE analyses across the mineralized horizon (from DDH 416, see Fig. 2 for location) show good correlations between all elements (Fig. 11b, c). Ru and Ir, and to lesser extent also Rh and Os, have positive intercepts at zero ppb Pt+Pd, probably due to the presence of alloys (Barnes et al. 2012). The average calculated composition of the sulfide fraction in the mineralized cumulate body (S≥0.2 wt%) is 6.2 wt% Ni, 1.8 wt% Cu, 4.2 ppm Pd, and 9.0 ppm Pt. Element correlations within the sulfide fraction are broadly similar to those in whole-rock data, with positive correlations between various metals. However, comparison of Ni and Cu contents in the sulfide fraction against the whole-rock S content shows an opposite behavior: Ni tenors (as well as Pt+Pd

Table 3 Examples of precious metal and Ni, Cu, and S analyses of mineralized cumulate body (MC) and barren cumulate body (BC) from the Lomalampi area

Sample Rock type DDH/ Depth	L11053334 Peridotite (MC) R416/43.90	L11053335 Peridotite (MC) R416/45.90	L07006927 Peridotite (MC) R416/39.90	L07006930 Peridotite (MC) R416/47.90	L07149454 Peridotite (BC) R426/11.80	L07149455 Peridotite (BC) R425/30.10
Au (ppb)	61.6	98.4	3.18	142	2.06	2.34
Ir	14.0	25.6	7.26	24.3	2.66	2.6
Os	7.38	4.21	3.23	11.6	2.85	3.8
Pd	316	613	108	671	17.4	3.15
Pt	768	1490	235	1340	18.6	5.64
Rh	16.1	33.7	9.18	29.3	1.29	b.d.
Ru	14.0	22.9	8.21	26.5	5.16	4.96
Re	1.60	1.27	n.d.	n.d.	1.21	1.22
Ni (ppm)	2,990	3,670	1,200	3,770	864	916
Cu	864	1,500	355	397	33	24
S	13,300	17,500	4,400	20,500	80	464

b.d. below detection limit, *n.d.* not determined

tenors) decrease with increasing S, whereas Cu tenors show a slight increase.

The primitive mantle-normalized multi-element pattern of the sulfide fraction in the Lomalampi ore body is more fractionated than other komatiite-hosted disseminated sulfide deposits and resembles those of komatiitic basalt-hosted Ni-Cu deposits such as Katinniq or Donaldson (Lesher 2007) (Fig. 12). The Lomalampi samples also lack the negative Ir and Pt anomalies that are persistent features of most komatiite-hosted sulfide deposits (Barnes 2004; Barnes 2006; Barnes

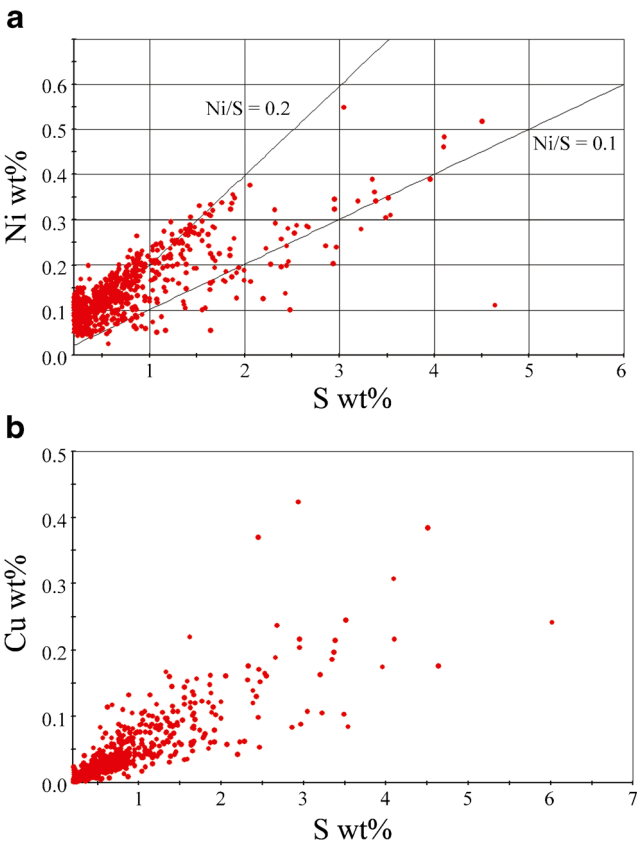

Fig. 9 **a** Sulfur vs. Ni and **b** Cu diagrams for whole-rock samples from the mineralized ultramafic body

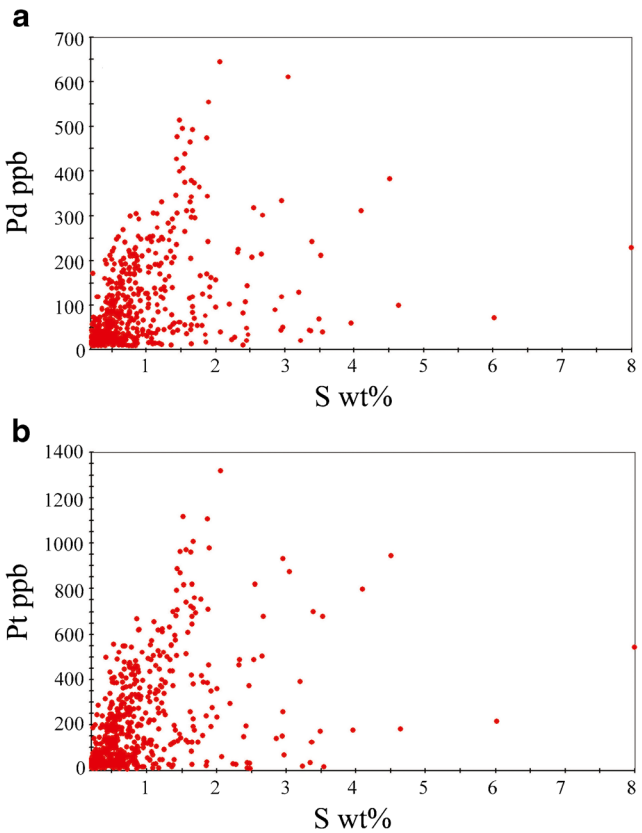

Fig. 10 **a** Sulfur vs. Pd and **b** Pt diagrams for whole-rock samples from the mineralized ultramafic body

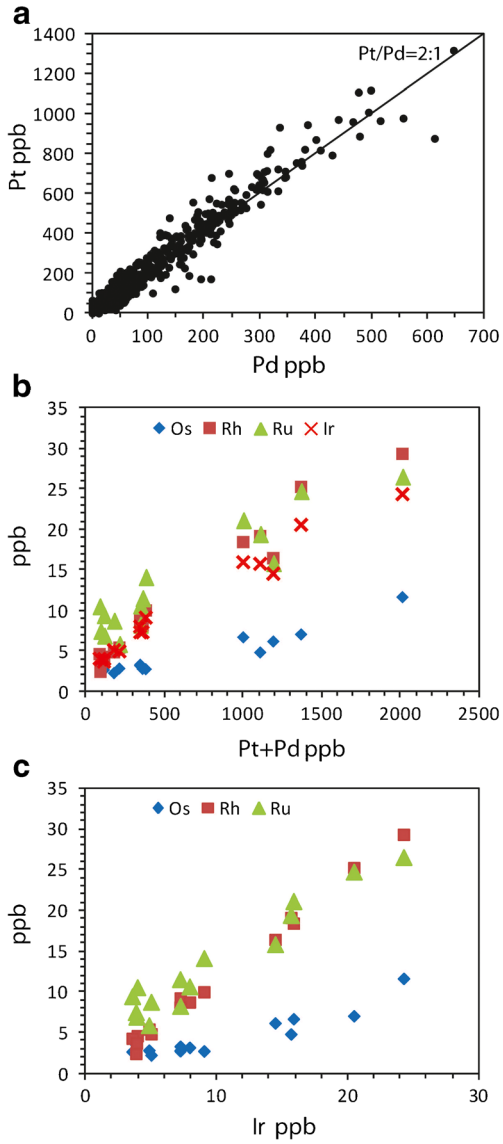

Fig. 11 **a** Pd vs. Pt for samples with ≥0.2 % S. **b** Correlations between Pt+Pd and Ir, Os, Ru, and Rh. **c** Correlations between Ir and Os, Ru, and Rh

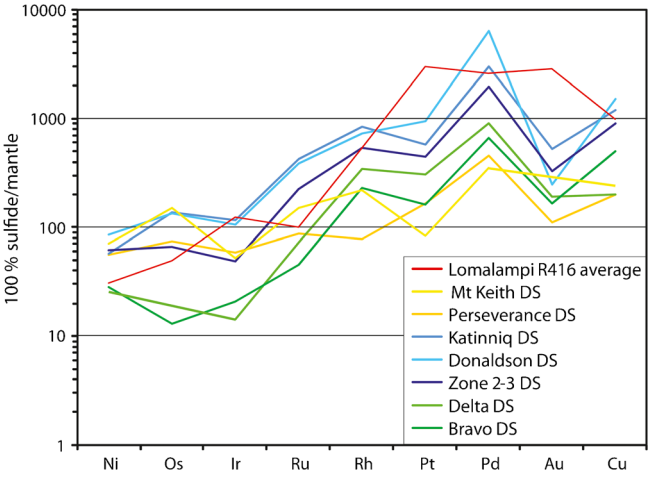

Fig. 12 Primitive mantle-normalized chalcophile element patterns (100 % sulfide) for Lomalampi and komatiite-hosted disseminated Ni-deposits from Western Australia (data from Lesher and Keays 2002) and Raglan area (data from Lesher 2007). Mantle normalization values from Barnes and Maier (1999)

et al. 2012). In comparison, the barren komatiitic body shows less fractionated PGE patterns and a Pt/Pd ratio closer to unity (1.3).

Sulfur isotopes

Figure 13 shows $\delta^{34}S$ data from the Lomalampi area and some dominantly komatiitic Ni-Cu-(PGE) deposits worldwide. Two sulfide separates were analyzed from mineralized samples, yielding $\delta^{34}S$ values of +10.5 and +9.8‰. Two mineralized whole-rock samples also yielded heavy $\delta^{34}S$ isotope compositions of +11.27 and +15.04‰. Two sulfide separates from sulfide-bearing country rocks, one representing sulfide-bearing sheared komatiitic volcanic rock 15 m below the contact of the mineralized cumulate and the other representing S-rich black schist at the lower contact of the mineralized cumulate, gave $\delta^{34}S$ values of +17.2 and +24.4‰, respectively. Sulfur isotope compositions were also determined for two whole-rock samples from sulfide-bearing country rocks representing amphibole-chlorite-biotite schist from the contact to the mineralized cumulate and a thin, homogeneous komatiitic lava 24 m below the mineralized cumulate contact. They showed $\delta^{34}S$ values of +21.8 and +17.01‰, respectively. No mass-independent sulfur isotope fractionation was observed in any of the analyzed samples as indicated by $\Delta^{33}S$ values of 0.016–0.059, which is consistent with their Paleoproterozoic age (cf. Johnston 2011). The obtained heavy sulfur isotope composition of the black schist sample is comparable to those measured earlier for sedimentary rocks from the Matarakoski Formation in the Kevitsa area (Grinenko et al. 2003).

Discussion

The Lomalampi mineralization has a unique composition among komatiite-hosted sulfide deposits in being S- and base metal-poor and relatively enriched in PGE, and especially in Pt (ESM 4). Compared to other S-poor reef-type PGE occurrences (e.g., Fred's Flow, Ontario, Wiluna and Mount Clifford, Western Australia, Stone et al. 1996; Fiorentini et al. 2007; Locmelis et al. 2009), the Lomalampi deposit has higher PGE and also Ni-Cu contents and is economically more significant. The average Pt/Pd ratio in the Lomalampi mineralized samples is 2.2, which is close to the chondritic value (Horan et al. 2003; Palme and O'Neill 2003) and higher than in other komatiite-hosted Ni-Cu-PGE deposits (Pt/Pd

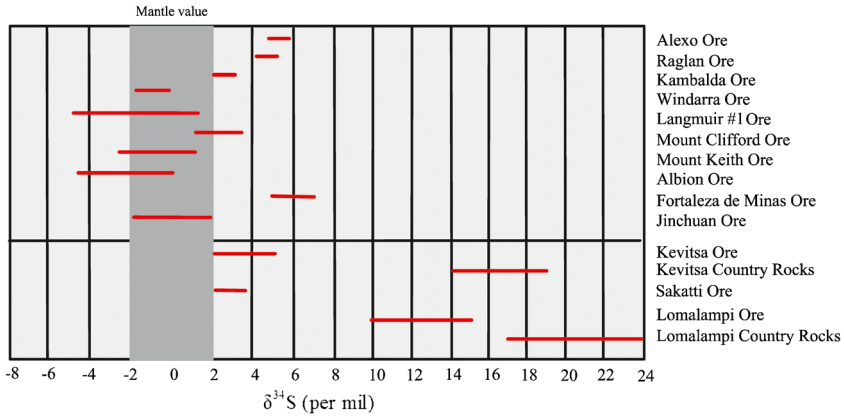

Fig. 13 Sulfur isotope compositions ($\delta^{34}S$) of the Lomalampi and other komatiite-hosted Ni-Cu-PGE deposits and Kevitsa Ni-Cu-PGE deposit. Reference data from Fiorentini et al. (2012), Choudhuri et al. (1997), and Grinenko et al. (2003)

0.5–0.66) (Lesher and Keays 2002; Fiorentini et al. 2010; Barnes and Liu 2012). In the case of the Lomalampi mineralization, the parental magma composition, magma/sulfide ratio (R-factor), and potential contamination with country rock material are among the most important factors to be taken into account when considering the genesis of the deposit.

Volcanology and geochemical features

The Lomalampi area hosts extrusive komatiitic to komatiitic basalts and cumulate bodies, whereas picrites, which are found is some other parts of the CLGL (e.g., Hanski et al. 2001a), have not been encountered. The volcanological character of the ultramafic bodies in the Lomalampi area is not clear. The bodies are differentiated, consisting of peridotites to pyroxenites, and the largest barren body has a gabbroic margin. Either these bodies are cumulates of associated komatiitic lava flows or they represent differentiated subvolcanic sills. Based on whole-rock analyses, the ultramafic bodies have almost similar compositions, representing Al-undepleted type primary magmas ($Al_2O_3/TiO_2 > 15$). However, barren ultramafic bodies contain MgO-enriched cumulates and show slightly higher Al_2O_3/TiO_2 than the mineralized body.

Establishing the parental magma composition of the Lomalampi ultramafic rocks is complicated because well-preserved rocks that might represent the liquid composition or primary olivine/pyroxene were not found due to metamorphic alteration. A melt inclusion study from the Jeesiörova area shows that the silicate liquids contained 10 to 22 wt% MgO (ave. 15 wt% MgO of seven samples) (Hanski and Kamenetsky 2013).

Crystallization of chromite is controlled by the composition of the magma, oxygen fugacity, temperature, and volcanic facies (e.g., Barnes 1998; Barnes and Fiorentini 2012). The Lomalampi komatiitic cumulates were derived from a chromite-saturated komatiitic liquid. The cumulate samples plot just below the trend of chromite-saturated liquids representing cotectic olivine-chromite crystallization under quartz-fayalite-magnetite buffer conditions (ΔQFM +1.44), whereas samples on the olivine-liquid mixing line (i.e., more magnesian liquid) are absent (Murck and Campbell 1986; Barnes 1998; Barnes and Fiorentini 2012) (Fig. 7a; see Barnes and Fiorentini 2012 Fig. 8a). It can be concluded that the Lomalampi cumulates crystallized from low-Mg komatiitic to komatiitic basalt liquids, in which the MgO content was somewhat less than 24 wt% MgO, which is the point where komatiitic melt reaches the chromite saturation surface at QFM (Barnes 1998).

Rare earth element patterns of rocks from the uncontaminated, barren cumulate bodies are almost flat ($(La/Sm)_{CN}$ is close to 1), whereas in the mineralized cumulate body, LREEs are clearly depleted ($(La/Sm)_{CN}$ is around 0.5). The mineralized body has similar REE patterns to those of komatiitic lavas in the Jeesiörova area (Hanski et al. 2001a, b), but the barren cumulate bodies represent a different type of komatiitic rocks in the area. These features, together with whole-rock geochemistry, show that the barren and mineralized cumulate bodies represent products of simultaneous komatiite-picrite magmatism in the Central Lapland Greenstone Belt and/or mixing of these magmas (e.g., Hanski and Kamenetsky 2013).

In terms of LREE, strong contamination signals can be seen in some samples from the barren cumulate bodies, whereas clear evidence for contamination has not been seen in the mineralized ultramafic body. Some mineralized samples show a weak LREE enrichment that could be a result of contamination by small amounts of LREE-rich country rock material. Positive La peaks in some cumulate samples are likely due to post-magmatic alteration. However, S isotope determinations ($\delta^{34}S$) from the mineralized ultramafic body show strongly positive values, far from typical mantle values (0±2 ‰) (e.g., Ripely 1999; Lesher and Keays 2002). S isotope measurements from country rock samples yielded even higher positive $\delta^{34}S$ values, compared to the cumulate samples. The strongly positive $\delta^{34}S$ values in the mineralized cumulate

body are evidently caused by mixing of magmatic and sedimentary sulfur in variable amounts, with approximately 50–60 % of the sulfur coming from a sedimentary source. The weak contamination signal seen in the whole rock and REE data combined with the strong contamination indicated by the S-isotope data suggests that the contamination did not involve large amounts of bulk country rock assimilation. Instead, the contamination took place through a more selective process, such as devolatilization of S-rich footwall metasediments. The addition of external sulfur played an important role in the genesis of the Lomalampi deposit, which is consistent with the current understanding on the genesis of komatiite-hosted Ni-Cu-PGE deposits.

Enrichment of chalcophile elements

Typical features of the Lomalampi disseminated sulfide deposit are the low Ni, moderate to high Cu and high Pt and Pd contents, low Ni/Cu ratio, and high Pt/Pd ratio. Table 4 shows the average and median composition and tenors of sulfide bearing samples (≥0.2 wt% S) and PGE-mineralized samples (≥100 ppb Pt+Pd). The sample population with >0.2 wt% S includes samples with elevated S contents but a low Ni-Cu-PGE content, whereas the PGE-enriched population represents the economically interesting samples.

Disseminated komatiite-hosted sulfide deposits from elsewhere, with similar sulfur contents to those at Lomalampi (0.2–3 wt%), tend to have higher Ni contents (0.5–1 wt%) and generally lower Cu contents (5–200 ppm) and lower Pt and Pd contents (typically between 50 and 300 ppb) (Barnes and Liu 2012; Barnes et al. 2012; Gole 2008). These differences are also reflected in the average metal tenors as shown in ESM 5.

The Lomalampi deposit shows a relatively low Ni tenor, elevated Cu tenor, and high Pt and Pd tenors. Some of the deposits in the Raglan area have similar Ni-Cu tenors (e.g., Delta, Bravo, ESM 5) and comparable or even higher Pd tenors (e.g., Zone 2–3, Donaldson, Katinniq), but lower Pt tenors (Barnes and Picard 1993; Barnes et al. 1997; Lesher 2007). The similarity between the deposits in the Raglan area and the Lomalampi deposit is also evident in the Ni/Cu vs. Pd/Ir diagram of ESM 6. Ni-Cu-PGE deposits hosted by komatiitic basalts tend to have higher Pd/Ir and lower Ni/Cu ratios than to komatiite-hosted deposits (Barnes and Maier 1999).

There are several processes that affect the final concentration of chalcophile elements in a magmatic sulfide deposit: (1) concentrations of the metals in the mantle, (2) degree of mantle melting and the presence of sulfide or alloy phase(s) in the mantle residue, (3) timing and style of possible contamination, (4) R-factor (mass ratio of silicate magma to sulfide liquid), (5) physical environment of the silicate magma during sulfide melt segregation, and (6) post-magmatic modifications.

Komatiitic melts are the product of high-degree partial melting of mantle; estimations vary generally between 30 and 60 %, whereas komatiitic basalts are produced by slightly lower degree of melting between 15 and 30 % (Lesher and Stone 1996; Lesher et al. 2001; Barnes and Maier 1999). A consequence of the high melting degrees is that all sulfur and associated highly incompatible elements present in the source rock (e.g., Pt, Pd and Cu) are dissolved in the silicate liquid. Estimations of the percentage of melting required to consume all the sulfur are variable; Barnes and Lightfoot (2005) give a minimum of 20 to 40 %, while modeling by Naldrett (2011) indicates that sulfur could be dissolved after 18 % of melting. Most estimates assume that the minimum amount of melting is 20–25 %. At this point, the resultant silicate magma would

Table 4 Average and median (in *brackets*) composition of sulfide mineralized samples (S≥0.2 %) and also PGE-mineralized samples (Pt+Pd≥100 ppb) from the ore cumulate

	Sulfide mineralized samples (S>0.2 wt%)		PGE mineralized samples (Pt+Pd>100 ppb)	
	Whole rock	100 % sulfide	Whole rock	100 % sulfide
Ni	1096 ppm	6.16 %	1386 ppm	6.16 %
	(890)	(6.04)	(1250)	(6.04)
Cu	446	1.77	599	2.06
	(266)	(1.53)	(406)	(1.84)
Pt (ppb)	191	9047	301	13,313
	(96)	(6840)	(253)	(12,320)
Pd	87	4183	138	4889
	(44)	(3136)	(108)	(4025)
Ni/Cu	5.15		4	
	(3.16)		(2.8)	
Pt/Pd	2.25		2.32	
	(2.13)		(2.17)	
N	663		392	

have its maximum Pt, Pd (i.e., PPGEs), and Cu concentrations, assuming that these elements are solely controlled by sulfides in the mantle and not affected by the presence of alloys (e.g., Pt-Fe). The IPGEs (i.e., Ir, Os and Ru) are controlled by more refractory phases such as mss, chromite, olivine, and IPGE alloys (e.g., Lesher and Stone 1996; Lorand et al. 1999; Pagé et al. 2012). Further melting, resulting in high-MgO komatiitic melts, would increase the concentration of Ni and IPGEs, whereas the concentrations of Pt, Pd, and Cu would be diluted. Due to lower degrees of partial melting, komatiitic basalt melts are thought to have slightly higher PPGE contents than high-Mg komatiites, producing PGE-enriched Ni-Cu deposits, such as in the Raglan area.

Estimates of the Pt and Pd contents of komatiitic parental melts are generally approximately 10 ppb for both elements (Barnes and Maier 1999; Barnes and Lightfoot 2005). Mantle melting modeling indicates even higher PGE concentrations in the melt at the point when all sulfur has been consumed: Pd contents could be up to five times that of primitive mantle, i.e., 15–20 ppb (Barnes and Lightfoot 2005; Naldrett 2011).

Estimates of the Pt/Pd ratio of komatiitic parental melts and also non-mineralized komatiites are mostly around unity, approaching that of the mantle source (Barnes and Maier 1999; Puchtel et al. 2004; Barnes and Lightfoot 2005; Mungall and Naldrett 2008; Barnes et al. 2009; Fiorentini et al. 2011), while komatiitic Ni-Cu-PGE deposits have commonly Pt/Pd ratios of approximately 0.5 (Fiorentini et al. 2010; Barnes et al. 2012). The discrepancy between the Pt/Pd ratio in the chondritic mantle and komatiitic melt has been explained by partial retention of Pt in the mantle by an alloy or a small amount of sulfides (Lorand et al. 1999; Bockrath et al. 2004; Barnes and Lightfoot 2005), by higher D values for Pd compared to Pt (Barnes et al. 1997), or by kinetic factors affecting the rate of diffusion of Pt from silicate melt into sulfide melt (Mungall 2002; Fiorentini et al. 2010; Barnes et al. 2012). The relatively low Pt/Pd ratios in komatiite-hosted sulfide deposits can likely be explained by relatively higher D of Pd than Pt with regard to sulfide liquid (Barnes et al. 1997).

Several features, such as whole-rock chemistry, composition of the sulfide fraction and various metal ratios of the Lomalampi deposit point to a low-MgO komatiite or even komatiitic basalt as the parental magma (as discussed above). The postulated relatively low MgO content of the parental magma and hence a relatively low degree of partial melting could result in somewhat higher PGE concentrations in the parent magma (≥10 ppb of both Pt and Pd) compared to komatiitic melt. However, the degree of melting must have been high enough to consume all sulfides present in the mantle.

Samples with low sulfur contents (<1000 ppm) from the non-mineralized part of the host cumulate have an average Pd content of 11 ppb and an average Pt content of 27.1 ppb (using 5-ppb concentrations for values below the detection limit of 10 ppb), resulting in a Pt/Pd ratio of 3.1 (median 2.5). This could indicate that the high Pt/Pd ratio is a primary magmatic feature inherited from the original silicate melt. High Pt/Pd ratios (around 2 or higher) have recently been reported in non-mineralized komatiitic rocks from the northern parts of the Central Lapland Greenstone Belt (Heggie et al. 2013). The 2.05-Ga Kevitsa intrusion close to Lomalampi (Fig. 1) hosts a disseminated Ni-Cu-PGE deposit with an average Pt/Pd ratio of 1.8 (Mutanen 1997). The recently discovered Sakatti deposit, in the same area (Fig. 1), also shows relatively high Pt/Pd ratios (1.6–2) in the disseminated portions of the deposits, while massive sulfides show Pt/Pd ratios close to unity (0.9–1) (Coppard et al. 2013). Some of the late Archean komatiite-hosted Ni-deposits in eastern Finland are also enriched in PGE, but they have much lower Pt/Pd ratios (0.4–0.5) (Konnunaho et al. 2015). Fiorentini et al. (2011) noted that komatiites from the Archean Youanmi Terrane have higher than average Pt/Pd ratios (1.2–1.4) and suggested that this reflects provincial heterogeneity of the mantle source. Similarly, the high Pt/Pd ratios of the abovementioned magmatic Ni-Cu-PGE deposits within the CLGB could reflect a regional mantle feature.

The R-factor, i.e., the weight ratio between silicate melt and sulfide melt, is often cited as a fundamental factor controlling metal tenors in magmatic Ni-Cu-PGE deposits (Campbell and Naldrett 1979 and references thereon). Estimated R-factor values for komatiitic Ni-sulfide deposits are generally between 100 and 500 (Lesher and Campbell 1993; Barnes et al. 2011) resulting in relatively low PGE-tenors of 500 to 3000 ppb Pd (Barnes 2006; Barnes et al. 2012), whereas for deposits hosted by komatiitic basalts, the estimated R-factors are between 300 and 1100 (Barnes and Picard 1993; Lesher 2007) resulting in considerably higher PGE tenors of more than 2000 ppb Pd and Pt in the Raglan massive to disseminated deposits (up to 25,000 and 6600 ppb, respectively) (Lesher 2007). R-factor modeling at Lomalampi was done using the following equation (Campbell and Naldrett 1979):

$$C_S = C_L D(R+1)/(R+D) \quad (1)$$

where C_S is the concentration of a metal in sulfide liquid, C_L is the concentration of a metal in silicate liquid, D is the partition coefficient between sulfide and silicate liquids, and R is the ratio of silicate liquid to sulfide liquid. Using the calculated sulfide liquid metal concentrations and the initial concentrations (C_L) of 15 for Pt and 10 ppb for Pd, R-factors generally fall between 500 and 1000 (Fig. 14). Similar results were obtained using Pt-Ir data from hole R416 (C_{LPt}=15 ppb, C_{LIr}=0.5 ppb) with the R-factors varying between ca. 700 and 1100. Nickel and copper gave best fits with melt concentrations of approximately 500 ppm for Ni and 75 ppm for Cu and D values of 150 for Ni and 400–500 for Cu. Modeled R-factor values are similar to those determined for the Raglan

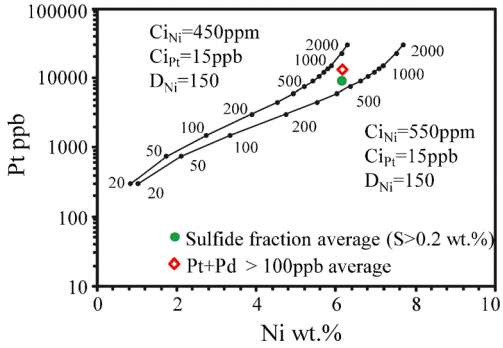

Fig. 14 R-factor model for Lomalampi using both sulfur mineralized (S≥0.2 wt%) and PGE-mineralized (≥100 ppb Pt+Pd) sample averages

deposits and provide further evidence for a komatiitic basalt to low-Mg komatiitic parental melt composition at Lomalampi.

The host-cumulate of the Lomalampi deposit has been altered to serpentine-chlorite±talc±amphibole rock as a result of regional metamorphism of the CLGB. More intense alteration toward the structural footwall has resulted in the formation of a talc±carbonate-rich zone. In many type II disseminated sulfide deposits, host-rock alteration has also affected the original, magmatic pyrrhotite-pentlandite-chalcopyrite paragenesis, often resulting in sulfide assemblages containing pentlandite, pyrite, millerite, heazlewoodite, or violarite. Replacement of pyrrhotite (and other Fe-containing sulfides) by magnetite is also common. These alteration features are thought to result from reaction with oxidizing fluids with concomitant S loss or gain (Groves et al. 1974; Barnes and Hill 2000; Barnes 2006; Barnes et al. 2009; Konnunaho et al. 2013). The preservation of the magmatic sulfide paragenesis, general lack of magnetite replacement, and good inter-element correlations between all six PGEs indicate negligible modification of the Lomalampi mineralization by hydrothermal fluids and testify to its magmatic origin. However, the observed decrease in Ni and PGE tenors in the most S-rich samples and corresponding slight increase in the Cu tenor could indicate more abundant input of external sulfur and possibly copper for the more S-rich samples, during the contamination event.

Conclusions

1. Komatiitic rocks of the Lomalampi area form a part of the Paleoproterozoic ultramafic magmatism of the Central Lapland Greenstone Belt, which has simultaneously produced komatiites, komatiitic basalts, and picrites as extrusives, intrusives, and sills. The ultramafic rocks are often closely associated with S-rich sedimentary rocks of the Matarakoski Formation, thus representing a favorable environment for magmatic sulfide deposits. Several Ni-Cu-PGE sulfide deposits are known to exist in the area (e.g., Lomalampi, Kevitsa, and Sakatti).
2. The Lomalampi area contains komatiitic extrusive formations (e.g., thin lava flows and hyaloclastites of Ti-enriched composition) and komatiitic cumulate bodies (Al-undepleted type). The exact nature of these cumulate bodies is not clear, i.e., whether they represent cumulate parts of lava flows or komatiitic sills. One of these cumulate bodies hosts type II PGE-(Ni-Cu) mineralization.
3. The known sulfide mineralization is associated with a predominantly peridotitic orthocumulate body derived from a low-Mg komatiite or komatiitic basalt melt, which was relatively enriched in PGE.
4. The mineralization is magmatic in origin and consists of pyrrhotite-chalcopyrite-pentlandite sulfide assemblages without strong signals of post-magmatic modification such as extensive sulfide replacement by magnetite. Palladium minerals occur with sulfides (40 %) and silicates (50 %), whereas the most important Pt mineral (sperrylite) occurs mainly within silicates (80 %).
5. The deposit is commonly sulfur- (0.4–2 wt% S) and base metal-poor (Ni<0.5 wt% and Cu<0.4 wt%) but is enriched in PGE (Pt+Pd>500 ppb). Ni/Cu is less than 10, which is typical for ores generated from low-Mg komatiite to komatiitic basalt. The chondritic Pt/Pd (around 2) is unique amongst komatiitic ore deposits. High Pt and Pd, and moderate Cu and low Ni tenors characterize the Lomalampi deposit, which is similar to disseminated Ni-Cu-PGE deposits in the Raglan area. R-factor modeling suggests relatively high R-factors between 500 and 1000, which are similar to those calculated for disseminated deposits in the Raglan area.
6. The mineralized ultramafic body shows only weak LREE enrichment due to country rock contamination, although this could be related to post-magmatic alteration. However, the $\delta^{34}S$ values of around 10 to 15‰ differ substantially from the mantle value (0±2‰). This provides evidence of only minor bulk assimilation of country rocks. Instead, it is proposed that addition of external sulfur and possibly also some copper occurred by devolatilization of S-rich country rocks. Most likely, these elements were derived from footwall black schists that contain 2 % S and 500 ppm of Cu, on average.
7. Early formed sulfides were most PGE rich and depleted Pt and Pd in the residual silicate magma. Addition of late S (and possibly some Cu) increased the sulfur content of the magma, but not the PGE or Ni contents, which is reflected in the somewhat lower Pt+Pd and Ni tenors of the more S-rich samples and negative correlations between the PGE-Ni tenors and S content, whereas Cu tenors show slight increase with increasing sulfur content.
8. The high Pt/Pd ratio of the Lomalampi deposit is a primary magmatic feature possibly related to mantle melting processes and/or regional-scale Pt/Pd heterogeneity in the mantle. Further evidence for this heterogeneity is

provided by the presence of other PGE-enriched, and at least in some cases also Pt-dominant, Ni-Cu sulfide deposits in the area (e.g., Kevitsa and Sakatti). This could indicate higher prospectivity for magmatic Ni-Cu-PGE deposits for the whole Central Lapland Greenstone Belt.

Acknowledgments Geochemical data for this study was provided by the Geological Survey of Finland. Geological Survey of Finland supported this work. We thank Viena Arvola from Geological Survey of Finland for preparing some of the figures and Bo Johanson at the research laboratory of the Geological Survey of Finland and personnel at the Mineral Processing Laboratory of the Geological Survey of Finland for the SEM-EDS analyses and images. Bernd Lehmann, Wolfgang Maier, Marco Fiorentini, and Stephen J. Barnes provided constructive and helpful reviews and comments.

References

Arndt N (2008) Komatiites. Cambridge University Press, New York

Augé T, Salpeteur I, Bailly L (2002) Magmatic and hydrothermal platinum-group minerals and base-metal sulfides in the Baula Complex, India. Can Mineral 40:277–309

Barkov AY, LaFlamme JHG, Cabri LJ, Martin RF (2002) Platinum-group minerals from the Wellgreen Ni-Cu-PGE deposit, Yukon, Canada. Can Mineral 40:651–669

Barley ME, Kerrich R, Reudavy I, Xie Q (2000) Late archean Ti-rich, Al-depleted komatiites and komatiitic volcaniclastic rocks from the Murchison terrane in western Australia. Australia. Aust J Earth Sci 47:873–883

Barnes SJ (1998) Chromite in komatiites, 1. Magmatic controls on crystallization and composition. J Petrol 39:1689–1720

Barnes SJ (2004) Komatiites and nickel sulfides ores of the black swan area, yilgarn craton, western Australia. 4. Platinum group element distribution in the ores, and genetic implications. Mineral Deposita 39:752–765

Barnes SJ (2006) Komatiite hosted nickel sulphide deposits: geology, geochemistry, and genesis. Soc Econ Geol Spec Publ 13:51–118

Barnes SJ, Fiorentini ML (2012) Komatiite magmas and sulfide nickel deposits: a comparison of variably endowed Archean terranes. Econ Geol 107:755–790

Barnes SJ, Hill RE (2000) Metamorphism of komatiite-hosted nickel sulfide deposits. In: Spry P, Marshall B, Vokes F (eds) Metamophosed and metamorphogenic ore deposits. Rev Econ Geol 11: 203–215

Barnes S-J, Lightfoot PC (2005) Formation of magmatic nickel sulfide ore deposits and processes affecting their copper and platinum group element contents. In: Hedenquist JW, Thompson JFH, Goldfarb RJ, Richards JP (eds) Economic Geology One Hundredth Anniversary Volume: 179–213

Barnes SJ, Liu W (2012) Pt and Pd mobility in hydrothermal fluids: evidence from komatiites and from thermodynamic modeling. Ore Geol Rev 44:49–58

Barnes S-J, Maier WD (1999) The fractionation of Ni, Cu and the noble metals in silicate and sulphide liquids. In: Keays RR, Lesher CM, Lightfoot PC, Farrow CEG (eds) Magmatic ore deposits and their application in mineral exploration, vol 13, Geol assoc Canada short course., pp 69–106

Barnes SJ, Often M (1990) Ti-rich komatiites from northern Norway. Contrib Mineral Petrol 105:42–54

Barnes S-J, Picard CP (1993) The behaviour of platinum-group elements during partial melting, crystal fractionation, and sulphide segregation: an example from the cape smith fold belt, northern Quebec. Geochim Cosmochim Acta 57:79–87

Barnes S-J, Boyd R, Korneliussen A, Nilsson LP, Often M, Pedersen RB, Robins E (1987) The use of mantle normalization and metal ratios in discriminating between effects of partial melting, crystal fractionation and sulphide segregation on platinum group elements, gold, nickel and copper: examples from Norway. In: Prichard HM, Potts PJ, Bowles JFW, Cribb SJ (eds) Geo-Platinum 87, Elsevier, pp 113–143

Barnes S-J, Zientec ML, Severson MJ (1997) Ni, Cu, Au, and platinum-group element contents of sulphides associated with intraplate magmatism: a synthesis. Can J Earth Sci 34:337–351

Barnes SJ, Wells MA, Verrall MR (2009) Effects of magmatic processes, serpentinization, and talc-carbonate alteration on sulfide mineralogy and ore textures in the Black Swan disseminated nickel sulfide deposit, Yilgarn Craton. Econ Geol 104:539–562

Barnes SJ, Godel BM, Locmelis M, Fiorentini ML, Ryan CG (2011) Extremely Ni-rich Fe-Ni sulfide assemblages in komatiitic dunite at Betheno, Western Australia: results from synchrotron X-ray fluorescence mapping. Aust J Earth Sci 58:691–709

Barnes SJ, Fiorentini ML, Fardon MC (2012) Platinum group element and nickel sulphide ore tenors of the Mount Keith nickel deposit, Yilgarn Craton, Australia. Mineral Deposita 47:129–150

Bockrath C, Ballhaus C, Holzheid A (2004) Fractionation of the platinum-group elements during mantle melting. Science 305: 1951–1953

Cabri LJ, LaFlamme JHG (1981) analyses of minerals containing platinum-group elements. In: Cabri LJ (ed) Platinum-group elements: mineralogy, geology, recovery. Can Inst Min Met, Spec Vol 23: 151–173

Campbell IH, Naldrett AJ (1979) The influence of silicate: sulphide ratios on the geochemistry of magmatic sulfides. Econ Geol 74:1503–1506

Chen Y, Fleet ME, Pan Y (1993) Platinum-group minerals and gold in arsenic-rich ore at the Thopson Mine, Thopsom Nickel Belt, Manitoba, Canada. Mineral Petrol 49:127–146

Choudhuri A, Iyer SS, Krouse HR (1997) Sulfur isotopes in komatiite-hosted Ni-Cu sulphide deposits from the Morro do Ferro Greenstone belt, southeastern Brazil. Int Geol Rev 39:230–238

Coppard J, Klatt S, Ihlenfeld C (2013) The sakatti Ni-Cu-PGE deposit in northern Finland. In: Hanski E, Maier W (eds) Excursion guidebook FINRUS, Ni-Cr-PGE deposits of Finland and the Kola Peninsula, 12th SGA Biennial Meeting, Mineral Deposit Research for a High-Tech World, 12–15 August 2013. Uppsala, Geological Survey of Sweden, Uppsala

Eilu P, Hallberg A, Bergman T, Bjerkgård T, Feoktistov V, Korsakova M, Krasotkin S, Lampio E, Litvinenko V, Philippov N, Sandstad JS (2013) Fennoscandian Ore Deposit Database. Online at http://en.gtk.fi/informationservices/databases/fodd/index.html

Fiorentini ML, Beresford SW, Grguric B, Barnes SJ, Stone WE (2007) A typical stratiform sulfide-poor platinum-group element mineralization in the Agnew-Wiluna Belt komatiites, Wiluna, Western Australia. Aust J Earth Sci 54:801–824

Fiorentini ML, Barnes SJ, Lesher CM, Heggie GJ, Keays RR, Burnham OM (2010) Platinum group element geochemistry of mineralized and nonmineralized komatiites and basalts. Econ Geol 105:795–823

Fiorentini ML, Barnes SJ, Maier WD, Burnham MC, Heggie G (2011) Global variability in the platinum-group element contents of komatiites. J Petrol 52:83–112

Fiorentini M, Beresford S, Barley M, Duuring P, Bekker, A, Rosengren N, Cas R, Hronsky J (2012) District to camp controls on the genesis of komatiite-hosted nickel sulfide deposits, Agnew-Wiluna Greenstone Belt, Western Australia: Insights from the multiple sulfur isotopes. Econ Geol 107:781–796

Gervilla F, Kojonen K (2002) The platinum-group minerals in the upper section of the Keivitsansarvi Ni-Cu-PGE deposit, northern Finland. Can Mineral 40:377–394

Gole M (2008) Metasomatic interaction between disseminated nickel sulfides and reduced metamorphic fluids, Honeymoon Well komatiite complex, Western Australia. Appl Earth Sci 177:112–124, **Transactions of the Institute of Mining and Metallurgy B**

Grguric BA, Seat Z, Karpuzov AA, Simonov ON (2013) The West Jordan deposit, a newly-discovered type 2 dunite-hosted nickel sulfide system in the northern Agnew-Wiluna belt, Western Australia. Ore Geol Rev 51:79–92

Grinenko LN, Hanski E, Grinenko VA (2003) Formation conditions of the keivitsa Cu-Ni deposit, northern Finland: evidence from S and C isotopes. Geochem Int 41:154–167

Groves DI, Hudson DR, Hack TBC (1974) Modification of iron-nickel sulfides during serpentinization and talc-carbonate alteration at Black Swan, Western Australia. Econ Geol 69:1265–1281

Hanski EJ (1992) Petrology of the Pechenga ferropicrites and cogenetic, Ni-bearing gabbro-wehrlite intrusions, Kola Peninsula, Russia. Bull Geol Surv Finland 367

Hanski EJ, Huhma H (2005) Central Lapland greenstone belt. In: Lehtinen M, Nurmi PA, Rämö OT (eds) Precambrian geology of Finland: key to the evolution of the Fennoscandian Shield. Developments in Precambrian Geology, vol 14. Elsevier, Amsterdam, pp 139–193

Hanski EJ, Kamenetsky VS (2013) Chrome spinel-hosted melt inclusions in Paleoproterozoic primitive volcanic rocks, northern Finland: evidence for coexistence and mixing of komatiitic and picritic magmas. Chem Geol 343:25–37

Hanski EJ, Huhma H, Rastas P, Kamenetsky VS (2001a) The Paleoproterotzoic komatiite-picrite association of Finnish Lapland. J Petrol 42:855–876

Hanski EJ, Huhma H, Vaasjoki M (2001b) Geochronology of northern Finland: a summary and discussion. In: Vaasjoki M (ed) Radiometric age determinations from Finnish Lapland and their bearing on the timing of Precambrian volcano-sedimentary sequences. Geological survey of Finland, special paper 33. Geological Survey of Finland, Espoo, pp 255–279

Heggie GJ, Barnes SJ, Fiorentini ML (2013) Application of lithogeochemistry in the assessment of nickel-sulphide potential in komatiite belts from northern Finland and Norway. Bull Geol Soc Finl 85:107–126

Hölttä P, Väisänen M, Väänänen J, Manninen T (2007) Paleoproterozoic metamorphism and deformation in central Lapland, Finland. In: Ojala VJ (ed) Gold in the central Lapland greenstone belt. Geological survey of Finland. Special paper 44. Geological Survey of Finland, Espoo, pp 7–56

Horan MF, Walker RJ, Morgan JW, Grossman JN, Rubin AE (2003) Highly siderophile elements in chondrites. Chem Geol 196:5–20

Huhma H (1986) Sm-Nd, U-Pb and Pb-Pb isotopic evidence for the origin of the Early Proterozoic Svecokarelian crust in Finland. Bull Geol Surv Finland 338

Johnston DT (2011) Multiple sulfur isotopes and the evolution of Earth's surface sulfur cycle. Earth Sci Rev 106:161–183

Juvonen R, Lakomaa T, Soikkeli L (2002) Determination of gold and the platinum group elements in geological samples by ICP-MS after nickel sulphide fire assay: difficulties encountered with different types of geological samples. Talanta 58:595–603

Koistinen E, Heikura P (2010) Mineral resource assessment and 3D modelling of the Lomalampi deposit, Sondakylä Finland. Geological Survey of Finland Report M19/3723/2010/50 (unpublished report)

Konnunaho JP, Hanski EJ, Bekker A, Halkoaho TAA, Hiebert RS, Wing BA (2013) The Archean komatiite-hosted, PGE-bearing Ni-Cu sulfide deposit at Vaara, eastern Finland: evidence for assimilation of external sulfur and post-depositional desulfurization. Mineral Deposita 48:967–989

Konnunaho JP, Halkoaho T, Hanski E, Törmänen T (2015) Kometiite hosted Ni-Cu-PGE deposits in Finland. In: Maier W, Lahtinen R, O'Brien H (eds) Mineral deposits of Finland, Elsevier (in press).

Lehtonen M, Airo ML, Eilu P, Hanski E, Kortelainen V, Lanne E, Manninen T, Rastas P, Räsänen J, Virransalo P (1998) Kittilän vihreäkivialueen geologia: Lapin vulkaniittiprojektin raportti. Summary: the stratigraphy, petrology and geochemistry of the Kittilä greenstone area, northern Finland: a report of the Lapland Volcanite Project, Geological survey of Finland, report of investigation 140 (in Finnish with english summary). Geological Survey of Finland, Espoo

Lesher CM (2007) Ni-Cu-(PGE) deposits in the Raglan Area, Cape Smith Belt, New Quebec. In: Goodfellow WD (ed) Mineral deposits of Canada: a synthesis of major deposit-types, district metallogeny, the evolution of geological provinces, and exploration methods. Geol Assoc Canada, Mineral Deposits Division, Special Publication No. 5, pp 351–386

Lesher CM, Campbell IH (1993) Geochemical and fluid dynamic modelling of compositional variations in Archean komatiite hosted nickel sulphide ores in Western Australia. Econ Geol 88:804–816

Lesher CM, Keays RR (2002) Komatiite-associated Ni-Cu-(PGE) deposits: geology, mineralogy, geochemistry and genesis. In: Cabri LJ (ed) The geology, geochemistry, mineralogy and mineral benefication of platinum-group elements. Can Inst Mining. Metall, CIM Spec. Vol. 54, pp 579–619

Lesher CM, Stone WE (1996) Exploration geochemistry of komatiites. In: Wyman DA (ed) Trace element geochemistry of volcanic rocks: applications for massive sulphide exploration. Geol Assoc Can, Short Course Notes 12, pp 153–204

Lesher CM, Burnham OM, Keays RR, Barnes SJ, Hulbert L (2001) Trace-element geochemistry and petrogenesis of barren and mineralized komatiites associated with magmatic Ni-Cu-(PGE) sulphide deposits. Can Mineral 39:673–696

Locmelis M, Barnes SJ, Pearson JN, Fiorentini ML (2009) Anomalous sulfur-poor platinum group element mineralization in komatiitic cumulates, Mount Clifford, Western Australia. Econ Geol 104:841–855

Lorand JP, Pattou O, Gros M (1999) Fractionation of platinum-group elements and gold in the upper mantle: a detailed study in Pyrenean orogenic lherzolites. J Petrol 40:957–981

Maier WD (2005) Platinum-group element (PGE) deposits and occurrences: mineralization styles, genetic concepts, and exploration criteria. Invited presidential review. J Afr Earth Sci 41:165–191

Maier WD, Lahtinen R, O'Brien (2015) Mineral Deposits of Finland. Elsevier (In press)

Mungall JE (2002) Kinetic controls on the partitioning of trace elements between silicate and sulfide liquids. J Petrol 43:749–768

Mungall JE, Naldrett AJ (2008) Ore deposits of the platinum-group elements. Elements 4:253–258

Murck BE, Campbell IH (1986) The effects of temperature, oxygen fugacity and melt composition on the behavior of chromium in basic and ultrabasic melts. Geochim Cosmochim Acta 50:1871–1887

Mutanen T (1997) Geology and ore petrology of the Akanvaara and Koitelainen mafic layered intrusions and the Keivitsa-Satovaara layered complex, northern Finland. Bull Geol Surv Finland 395, 233 p

Mutanen T, Huhma H (2001) U-Pb geochronology of the Koitelainen, Akanvaara and Keivitsa layered intrusions and related rocks. In: Vaasjoki M (ed) Radiometric age determinations from Finnish Lapland and their bearing on the timing of Precambrian volcano-sedimentary sequences, Geological Survey of Finland. Special Paper 33. Geological Survey of Finland, Espoo, pp 229–246

Naldrett AJ (2004) Magmatic sulfide deposits: geology, geochemistry and exploration. Springer Verlag, Berlin-Heidelberg

Naldrett AJ (2011) Fundamentals of magmatic sulphide deposits. In: Li C, Ripley E (eds) Magmatic Ni-Cu and PGE deposits. Geology, Geochemistry, and Genesis. Rev. Econ. Geol. Vol 17, pp 1–51

Pagé P, Barnes S-J, Bédard JH, Zientek ML (2012) In situ determination of Os, Ir, and Ru in chromites formed from komatiite, tholeiite and boninite magmas: implications for chromite control of Os, Ir and Ru during partial melting and crystal fractionation. Chem Geol 302–303:3–15

Palme H, O'Neill HSC (2003) Cosmochemical estimates of mantle composition, in: Carlson R.W. (Ed.), The Mantle and Core. Treatise on Geochemistry Vol. 2, pp 1–38

Puchtel IS, Humayun M, Cambell AJ, Sproule RA, Lesher CM (2004) Platinum group element geochemistry of komatiites from the Alexo and pyke Hill area, Ontario, Canada. Geochim Cosmochim Acta 68: 1361–1383

Ripely ME (1999) Systematics of sulphur and oxygen isotopes in mafic igneous rocks and related Cu-Ni-PGE mineralization. In: Keays RR, Lesher CM, Lightfoot PC, Farrow CEG (eds) Dynamic processes in magmatic ore deposits and their application in mineral exploration. Geol Assoc Can Short Course Notes 13:133–158

Räsänen J, Huhma H (2001) U-Pb datings in the Sodankylä schist area, central Finnish Lapland. In: Vaasjoki M (ed) Radiometric age determinations from Finnish Lapland and their bearing on the timing of Precambrian volcano-sedimentary sequences, vol 33, Geological Survey of Finland, special paper. Geological Survey of Finland, Espoo, pp 153–188

Simonen A (1980) The Precambrian in Finland, vol 304, Bull Geol Surv Finland. Geological Survey of Finland, Espoo

Stone WE, Crocket JH, Fleet ME, Larson MS (1996) PGE mineralization in Archean volcanic system. Geochemical evidence from thick, differentiated mafic-ultramafic flows, Abitibi greenstone belt, Ontario, and implications for explorations. J Geochem Explor 56:237–263

Studley SA, Ripley EM, Elswick ER, Dorais MJ, Fong J, Finkelstein D, Pratt LM (2002) Analysis of sulfides in whole rock matrices by elemental analyzer-continuous flow isotope ratio mass spectrometry. Chem Geol 192:141–148

Törmänen T, Heikura P, Salmirinne H (2010) The komatiite-hosted Lomalampi PGE-Ni-Cu-Au deposit, Northern Finland. Geological Survey of Finland Report M19/3723/2010/52 (unpublished report)